TOWARD A RESPIRATOR CONTROL SYSTEM

BY

JOHN PETER SCHILL

B.S., University of Illinois, 1965
B.S., University of Illinois, 1965
M.S., University of Illinois, 1969

THESIS

Submitted in partial fulfillment of the requirements
for the degree of Doctor of Philosophy in Electrical Engineering
in the Graduate College of the
University of Illinois at Urbana-Champaign, 1976

Urbana, Illinois

TOWARD A RESPIRATOR CONTROL SYSTEM

John Peter Schill, Ph.D.
Department of Electrical Engineering
University of Illinois at Urbana-Champaign, 1976

This dissertation deals with the physiological basis for a control system for a respirator and its formulation for the design using optimal control theory.

The physiology of a patient who requires a respirator is deranged in a sufficiently unique manner as to make a general complex modeling impractical. This also eliminates the use of the general respiratory models of Grodins, Milhorn and others which are based upon a normal individual. A basic approach is taken emphasizing the gas exchange function of the human respiratory system and the maintenance of this exchange through proper use of pulmonary mechanics. A model that is amenable to application control theory is developed and justified.

Optimal control theory is applied to the dynamic equations of the model to yield design equations (control laws) of a controller. However, to design a controller that can be sufficiently inexpensive as to be available to a large portion of the patient population, it is necessary that control law be implementable on a microprocessor or a small mini-computer. Therefore, several different formulations of the control problem are considered and comparisons made. Specifically, the continuous formulation of the control problem for both time optimal and quadratic performance indices, sampled-data formulation for both time optimal and quadratic performance indices and the continuous time optimal maximum principle formulation are considered.

Finally, the implementation and future enhancements are discussed.

TABLE OF CONTENTS

LIST OF TABLES

LIST OF FIGURES

1. INTRODUCTION AND PROBLEM DEFINITION

The inability to "breathe adequately" is an experience that everyone has had at some time in their life and usually has not forgotten. Experiences such as swimming underwater or "having the wind knocked out of you" are of a short-term nature and, in a sense, "normal" episodes of lack of breath-dyspnea. These can be resolved by simply changing one's environment—leaving the water—or by resting. Other acute forms of inadequate ventilation of a more serious nature are the result of traumatic events such as drowning or electrocution. If treated in time, these forms of respiratory insufficiency can be resolved by artificial respiration, such as mouth-to-mouth resuscitation, with or without oxygen supplementation, as required. Other insufficiencies of longer duration require prolonged support of the respiratory processes such as an oxygen tent or a respirator. Treatment with an oxygen tent implies that the patient can physically (or mechanically) breathe "normally", but that his ability to diffuse oxygen across his lung membranes may be impaired. Thus, an enriched oxygen environment is required to overcome this impairment. Other patients cannot breathe physically due to an inability mechanically to force the air into and out of the lungs even though their ability to diffuse oxygen across the lung membranes is more or less intact. These patients require mechanical respirators to support the work of breathing—the physiological energy expended to promote the process of breathing.

The proper use of a respirator (ventilator) requires the close supervision by medical personnel to insure that it is functioning properly. This supervision involves the determination of the necessary ventilation

required to maintain medically determined blood gas concentrations through use of quantitive measures, such as the concentrations of carbon dioxide and oxygen in the blood, or qualitative measures, such as the blueness of the patient's skin.

Although the need for respirator control in one form or another has been with us for decades, it was not until 1954 that Radford [1] developed a nomograph to estimate the proper respirator control settings to maintain the necessary ventilation for the patient. This nomograph uses the patient's weight and sex to determine the amount of air inspired per breath (tidal volume) and the number of breaths per minute (rate) for the necessary ventilation. This nomograph, although a major and useful medical achievement, is based upon population norms and must be corrected for many special conditions such as altitude, obesity, or the presence of a fever. Even with the nomograph and present technology, one nameless surgeon describes the management of a patient on a respirator as being analogous to flying cross country with only telephone poles and past experience as navigation aids. Since individual respiratory requirements consistently vary beyond those given by this nomograph, it is evident that there is a need for a respirator control system that is adaptable to the patient's individual respiratory needs. Such a control must be simple and relatively economical to be generally useful. In addition, it should require no invasive transducers (transducers that penetrate the body's surface) to sense gas concentrations, or other input variables.

The purpose of this dissertation is to develop the background for the implementation of a prototype respirator control system. To provide

the necessary introduction for a respirator control, Section 1.1 contains discussion of respirators—their types, operation and use. Next a discussion of the respirator control will be presented. Section 1.2.1 defines the problem of respiratory control. The human control system is discussed with emphasis on its control mechanisms in Section 1.2.2, followed by a review of previous attempts of providing an external means of the regulation of human and animal respiration and identify a different approach.

1.1 Respirators

The treatment of respiratory disease is largely a mechanical problem—one of causing the lungs to be ventilated properly. As early as the second century A.D., the Greek physician Galen recognized that it was the weight of the atmosphere that forced air into the lungs when the volume of the chest was enlarged by the expansion of the thorax. The pneumatic characteristics of the lungs determine if the ventilation is sufficient to provide the necessary gas exchange. The types of respirators can be identified by their method of providing "the weight of atmosphere" for sufficient gas exchange.

The first respirators were used to assist patients with respiratory paralyses such as poliomyelitis. Initially, they were of the tank type (iron lung or Drinker-type) which enclosed all but the head of the patient. The internal pressure of the tank was varied in such a manner as to cause the alternative positive and negative pressure gradients across the lungs to cause inspiration and expiration. These iron lungs functioned well for the paralyzed patient in a hospital room or at home, but proved inadequate in the surgical operating room. Such iron lungs were of no use due to their size, weight, and structure, in addition to being difficult to operate during any electrical power failure. Some of these surgical problems were circumvented by the development of a "negative" pressure operating room—Sauerbruch's room—which was used to aid the respiration of anesthesized surgical patients during surgical operations [2].

From these cumbersome methods have evolved the simpler and more efficient methods. The most common is the use of intermittent positive

pressure (IPP) ventilation (IPPV) at the patient's mouth. This method recognizes the basic principle that the lungs can be inflated by a positive external pressure. Instead of changing the patient's surrounding environmental pressure, as with the iron lung or Sauerbrunch room, air is forced into the patient's lungs using a positive pressure gradient. The expired air is found from the lungs by the restoring elastic force of the lungs and diaphragm, like a deflating balloon. This technique has permitted the construction of a portable lightweight respirator which can function both in the surgical suite as well as the patient's room (or even his home).

Although the use of IPPV is the most common form of respiratory aid, there are many other methods. These are concisely discussed in Nunn [3] and Grogono and Byles [4]. Due to the predominant use of IPPV, the remaining discussion will be confined to IPP types of respirators.

Pulmonary ventilation of the lungs can be represented by a simple electrical analog in the form of an RC circuit. Electrical current represents the airway flow; the voltage is the analogue of airway pressure as shown in Fig. 1 [5-8]. The importance of airway resistance and compliance (pneumatic capacitance) will be discussed subsequently.

There are two basic types of IPP respirators: constant-pressure (represented by a constant voltage) and constant-flow (represented by a constant current). The constant-flow, also known as volume-limited or volume-preset, respirator is analogous to a current source, I_F, during the inspiratory portion of the breathing cycle. Such machines deliver very precise volumes of inspired air, but the peak pressure of the resultant air flow is dependent upon the pneumatic time constant represented by RC. The constant-pressure, also known as a pressure-controlled or

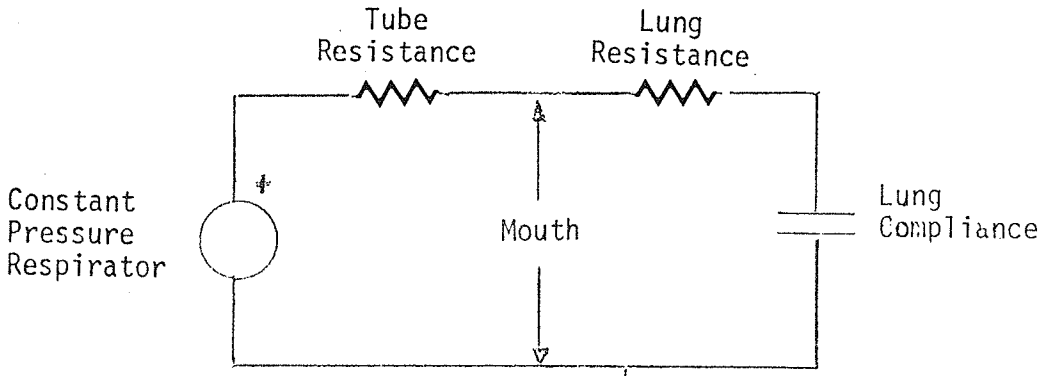

This respirator is pressure controlled.
It delivers inspired air at a constant pressure.
The flow rate is dependent upon the pneumatic time constant.

Figure 1a. Constant pressure regulator equivalent circuit.

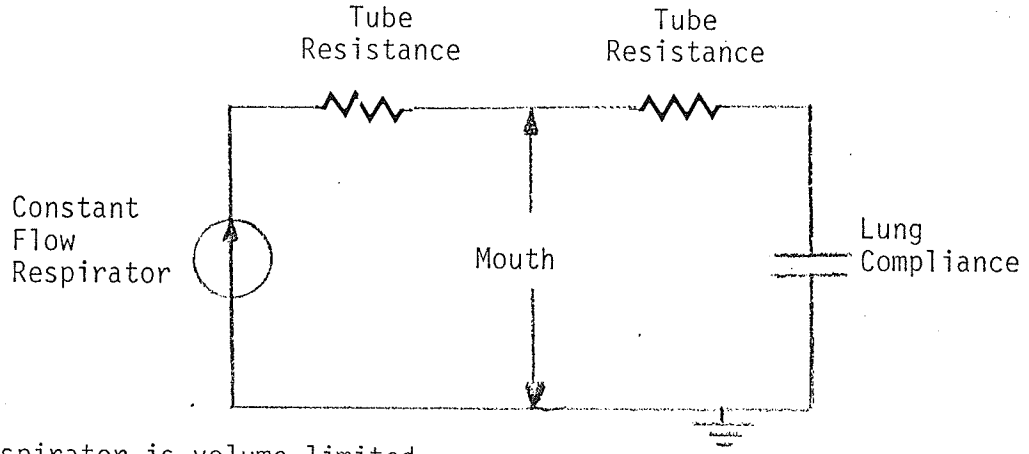

This respirator is volume limited.
It delivers a precise volume of inspired air.
The peak pressure is dependent upon the pneumatic time constant.

Figure 1b. Constant flow respirator equivalent circuit.

pressure-limited, respirator is analogous to a constant voltage source, V_F, and provides a constant pressure gradient at the mouth causing the air to flow into the lungs. The pressure setting is precise, but the rate of air flow into the lungs is dependent upon the pneumatic time constant. This property causes the actual volume of inspired air received by the patient to decrease with an increased airway resistance or decreasing compliance and to increase with an increase in compliance. There are other types of IPP respirators which act like variable pressure or flow sources. These types will not be discussed here. The reader is referred to Wald et al. [9] and Moore et al. [10] for a more complete discussion of these types of respirators.

In this dissertation, no distinction will be made between the pressure- and volume-controlled ventilators. Although some argue that these ventilators can be made to perform identically [12] or that it is more important to understand the details of operation of any ventilator rather than the simple selection of type [13], present clinical practice seems to favor the volume-controlled respirator. However, the state of the art of respirators changes frequently making any discussion a function of present technological development and clinical practice. Therefore, the use of the term respirator will be confined, unless otherwise specified, to a generic IPPV that could be either volume or pressure controlled.

To complete the discussion of respirators, additional comment is needed on the clinical use of respirators or respirator management. There are several excellent books and monographs describing respirator management in detail [2, 10, 13, 14]. Basically, the physician determines

the amount of carbon dioxide output and the inspired oxygen required to maintain the desired levels through blood gas concentration measurements. From these, using the Radford nomograph and clinical experience, he can estimate the rate and volume (per breath) and the gas concentrations of the inspired gas necessary to stabilize the patient's blood gas concentration levels at a desired value. Again, the Radford nomograph provides an approximation of the correct volume and frequency of respiration. But, a variety of additional factors, such as activity, obesity and fever, must be considered. If the physician is fortunate, he has equipment to measure the pneumatic characteristics of the patient's lungs and airway, as well as the diffusibility of CO_2 and O_2 across the air sacs or alveoli of the lungs. Hilberman, Patitucci and Peters [16], Osborne and associates [17], and Turney et al. [18] provide good discussions of such equipment. These additional measurements provide a refinement of, and sometimes change greatly, the estimates of rate, volume, and gas concentrations required for proper ventilation. In the critically ill patient, the drawing of blood for gas concentration analysis provides additional trauma. As will be discussed in more detail in Chapter 2, much information can be obtained about the blood gas concentrations from the gas concentrations and pressure and flow characteristics of the gases at the patient's mouth. This minimizes blood withdrawals for gas concentration analysis. This provides the control system with its primary source of information while only infrequent blood gas measurements are used to refine the estimate of proper ventilation.

1.2 Respiratory Control

We breathe to promote gas exchange with the whole body, just as the gastro-intestinal system promotes liquid and solid exchange. Consumables enter and wastes exit via these systems. A control system is needed to ensure that the body's needs for this gas exchange are adequately met. For the respiratory control system, "adequate ventilation" is the criterion.

1.2.1 Definition of the respiratory control problem

Before any discussion of respiratory control, it is necessary to define what is meant by adequate ventilation. Adequate ventilation "will insure satisfactory levels of both oxygen and carbon dioxide in the arterial blood, under prevailing conditions of barometric pressure, composition of the inspired gas, deadspace, distribution, shunting, diffusing and metabolic activity of the patient" [3]. This means that these satisfactory levels of blood gases, defined empirically, must be maintained by consideration of the physical properties of the inspired gases (barometric pressure and composition), physical properties of the lungs for gas exchange* and body requirements for gas exchange (metabolic activity). The human respiratory control system, in essence, is a state regulator type system controlling ventilation to maintain "preset" levels of carbon dioxide and oxygen, which may be defined as states. This form of ventilation has been suggested as meeting a minimum energy-type criterion [19-21].

---

*The following physical properties are: (1) deadspace — areas of the lungs where air enters, but no gas exchange takes place; (2) distribution of the gases within the lungs; (3) shunting — areas of the lungs through which blood passes, but no gases are exchanged; and (4) diffusion — the ability of the lung membrane to support gas diffusion between air and blood (Fig. 2).

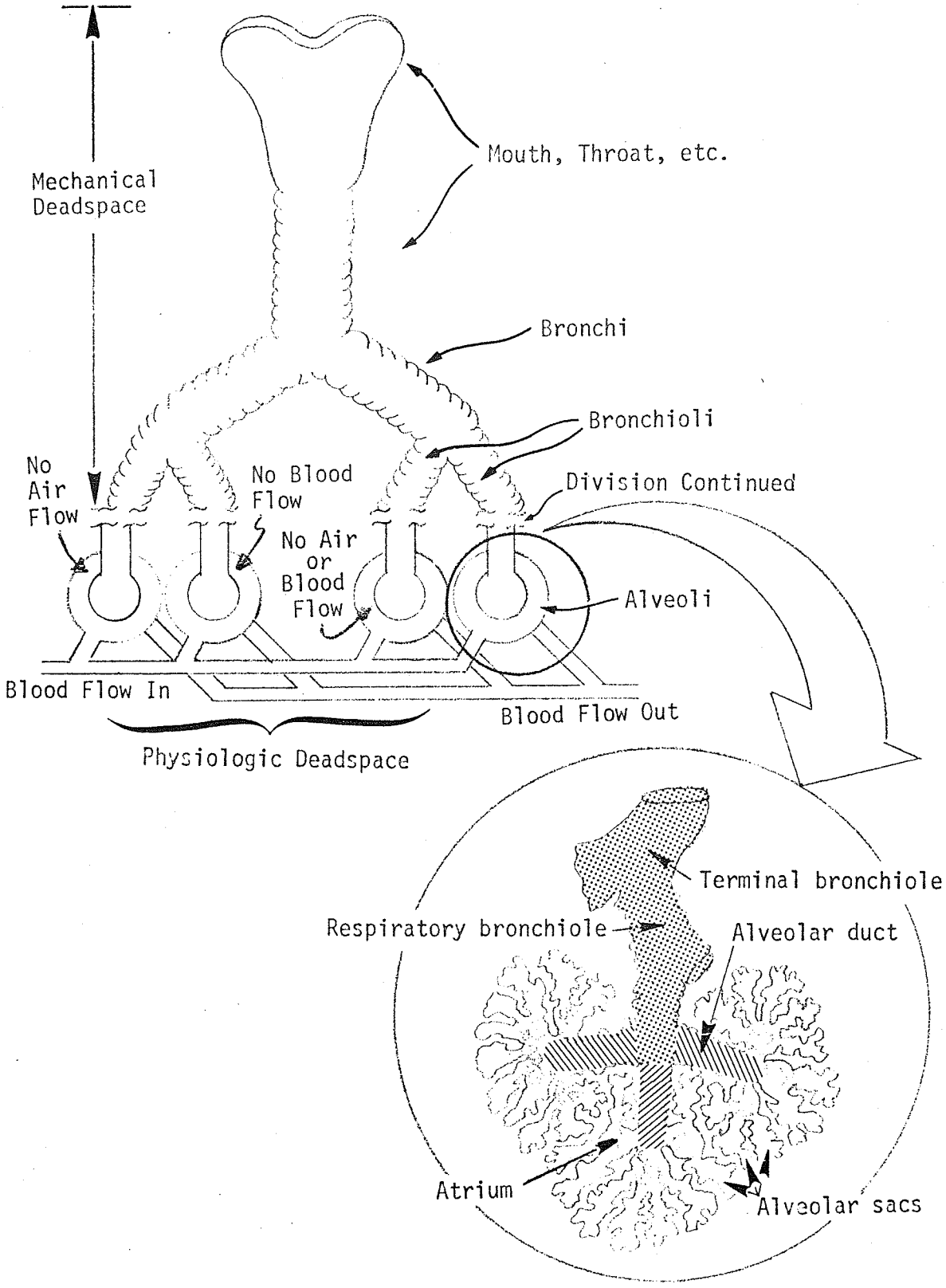

Figure 2. Anatomical schematic of human pulmonary system emphasizing deadspace definition.

Table 1 defines the symbols to be used in this report. The primary symbols represent quantities; the secondary symbols are used as subscripts which denote either the location of the particular measured quantity or the measurement condition. The primary symbols, F and P, change meaning depending upon the context indicated by the presence or absence of a subscript. For example, $F_I co_2$ means the fractional concentration of inspired carbon dioxide, whereas F alone represents the airway flow (usually as a function of time). Note that Q and V represent volumes of liquid and gas, respectively, and their time rate of change are denoted by dots above them, e.g., $\dot{Q}$ and $\dot{V}$. Similarly, the subscript T has contextual meaning, e.g., W_T is total work, but V_T is tidal volume. The context should eliminate any ambiguities in the meaning of the symbols.

1.2.2 Human respiratory control

Respiration is controlled by neural impulses which originate within the lower brain (medulla) and are transmitted to the chest cavity (thorax) and diaphragm to govern the rate and tidal volume. The basic inputs for the respiratory center are neural signals transmitted from peripheral or central sites in the body. There are two sources of these signals. The first source of signals is nonchemical in nature. These signals originate from mechanical sensors such as the stretch receptors in the lungs or from other neural sources such as emotion or voluntary control.

The second source of signals is chemical. Chemoreceptors are located centrally at or near the respiratory center and peripherally in the carotid and aortic bodies, and at other less important peripheral sites. The central chemoreceptors are primarily sensitive to concentrations

TABLE 1

PHYSIOLOGICAL SYMBOL DEFINITION

PRIMARY SYMBOLS		SECONDARY SYMBOLS	
C	content of a gas in liquid	A	alveolar
c	equivalent compliance	a	arterial
D	diffusing capacity of lungs for a given gas	Aa	alveolar arterial difference
F	the fractional concentration in airway (with subscript)	B	barometric pressure
F	flow rate in airway (without subscript)	c	capillary
$\overline{F}$	mean fractional concentration	$\bar{c}$	mean capillary
f	respiratory frequency	D	deadspace
P	partial pressure for a gas in airway (with subscript)	Dan	anatomical deadspace
P	total airway pressure (without subscript)	Dm	mechanical deadspace
$\overline{P}$	mean pressure	Dp	physiologic deadspace
Q	volume of blood	E	expiratory
$\dot{Q}$	volume of blood/unit time	Ee	end-expiratory
R	respiratory ratio	I	inspiratory
r	equivalent respiratory resistance	Ie	end-inspiratory
S	% saturation of Hb with O_2	M	minute (average over a minute)
V	volume of gas	R	resistive
$\dot{V}$	gas volume/unit time	T	tidal, or total
W	work	v	venous
α	conversion factor from ambient to STPD 862	$\bar{v}$	mixed venous
		VTPS	body temperature and pressure saturated with water vapor
		STPD	0^{o} C., 760 mm Hg

of carbon dioxide and hydrogen ions in the cerebro-spinal fluid and the cerebral blood. The carotid body, located in the neck, and the aortic body, located in the main artery from the heart, are primarily sensitive to oxygen concentration, although under certain conditions they are sensitive to carbon dioxide and hydrogen concentrations. A more detailed discussion of chemoreceptors can be found in Comroe [22] and DeJours [23].

For this discussion, the human respiratory control system (Fig. 3) may be functionally divided into two separate, but highly interactive, control systems: the chemical control system (CCS) and the external ventilation control system (EVCS). The function of the CCS is primarily to determine the required alveolar ventilation and to control internal systems to achieve that ventilation. The EVCS controls the body's interface to the air.

First consider the CCS, since most of the research has been done in this area. In 1946, Gray [24] first outlined the basis of a respiratory feedback control system. Later he and Grodins with several associates [25] formulated the first model of the CCS which provided an accurately productive simulation. Since then there have been many models developed, each incorporating some improvements over the previous model.

Before discussing them, it will be useful to examine their common elements. All the models subdivide the body into compartments. These compartments are characterized by the following:

1. They produce or absorb gases at a specific rate.
2. They contain concentrations of a specific gas in dissolved form, either within liquids or solids. These concentrations can be

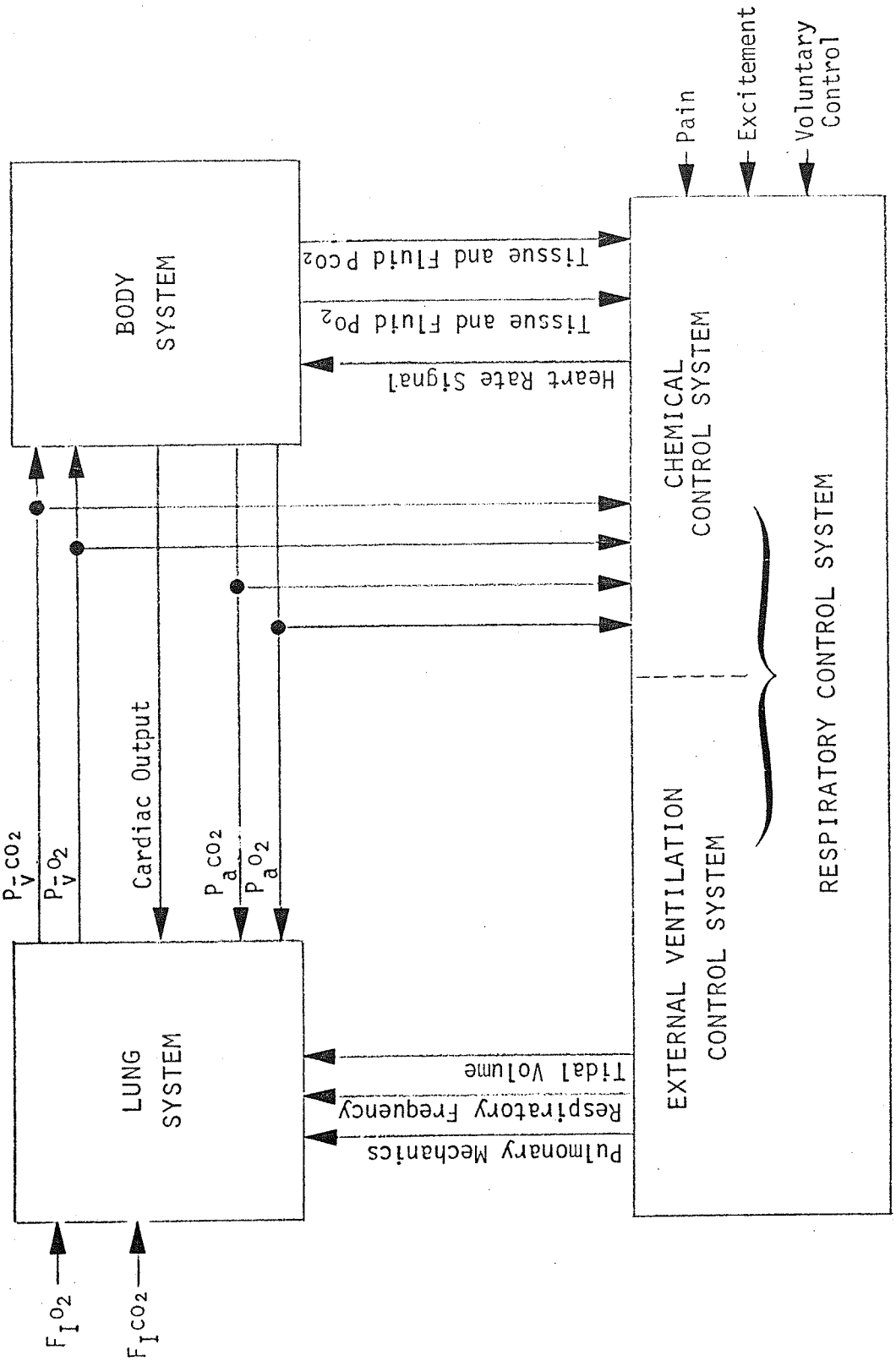

Figure 3. Human respiratory control system.

dissociated back into gaseous form. The relationship between the concentration of dissolved gas and the equivalent partial pressure of the free gas is called the gas's dissociation curve. Its shape is dependent upon the concentration of other gases, the pH and the temperature. A good theoretical discussion of oxygen's dissociation curve has been presented by Mikic, Benn and Drinker [26].

3. They exchange the gases with other compartments.

In addition to the compartments, the circulatory system is treated like a compartment since it exchanges gases with other compartments and provides the means of transport (and the representative time delays in the model) of the gases between compartments. For the gases to be exchanged between a body compartment and the circulatory system, blood must pass through the tissue of the body compartment. This passage is called perfusion and is probably the most important factor determining the parametric values of all gas exchange models. The last components in the system are the chemoreceptors. They are represented by nonlinear elements which relate the gas concentrations and the pH to the level of ventilation required to maintain homeostasis. Figure 3 illustrates the basic concept of the CCS without specifically identifying individual elements.

There are several reviews of the CCS models [27-29]. With the increased availability of the digital computer, improved mathematical techniques, and advances in transducer technology in the last ten years, models of respiratory control have flourished. These models have typically increased in both complexity and generality from the rather simple and

specific first model. In 1966, Yamamoto and Raub [27] divided these models into three groups. Their grouping is still quite applicable. The first group is characterized as improvements on Grodins' first model [25]. In 1960, Defares et al. [30] (later reported in more detail [31]) improved the first model by making two modifications to enhance the model's transient response to CO_2 changes. Both these models only considered the control of CO_2. A later model of Grodins and James [32] extends the model further to consider a controller which has dynamic characteristics which differ from its static ("steady-state") characteristics in order to try to simulate drastic change in breathing induced by exercise. Further improvements in computer technology and physiological information enabled Grodins and associates to revise the model even further in 1967, to include the regulation of oxygen [33]. Other offshoots of Grodins' first model include works of Priban [34, 35], Hey et al. [36], and Mathews et al. [37].

The second group of models were developed more or less independently of Grodins' efforts. Models in this group began by consideration of the phenomena of Cheyne-Stokes breathing, which consists of cycles of gradually increasing tidal volume followed by gradually decreasing tidal volume. Horgan and Lange [38] built their model primarily around the carbon dioxide and oxygen exchanges and the circulatory time delays. Later efforts refined the model's predictive capability [39] and added the influence of a carbon dioxide chemoreceptor in the cerebral spinal fluid [40].

The third group of models was based on a paper of Milhorn et al. in 1965 [41]. This group extends the existing work of Grodins and Defares by the addition of the oxygen portion of the system, providing nonlinear

dissociation curves in place of the linear ones, and including the time lags suggested by Horgan and Lange. There have been several enhancements incorporating additional physiological data [42-44].

As Milhorn and Brown [42] have pointed out, the major difficulty in the predictive capability of these models has been lack of information about the location and number of the chemoreceptors as well as their response to stimuli which create the ventilatory response. However, the steady-state (nearly static) operation of the human respiratory controller, and hence the CCS, may be taken as a function of known variables of known sites in the control loops. For an automated external respiratory controller, this means that a simple model will be well behaved if its operation is considered over a sufficiently long period.

The CCS determines the required level of alveolar ventilation, but the alveolar ventilation is only a part of the total ventilation as observed at the patient's mouth. This tidal ventilation is controlled by the external ventilation control system to achieve the required alveolar ventilation. The alveolar ventilation ($\dot{V}_A$) can be related to the minute ventilation ($\dot{V}_M$) by the following equation:

$$\dot{V}_A = (V_T - V_D) \times f = \dot{V}_M - V_D \times f \qquad (1\text{-}1)$$

where V_D is the deadspace. Note that this equation is a steady-state expression using mean values. From this equation, we see that the EVCS can adjust the frequency, tidal volume, and a portion of the deadspace to provide the necessary alveolar ventilation.

As with other types of optimal control systems, the EVCS also operates to minimize a cost functional. For the EVCS at a particular

alveolar ventilation, the efficiency of the gas exchange is maximized at a minimized cost in expended energy. This expended energy is in the form of oxygen consumption, carbon dioxide elimination, and available chemical energy required for the ventilatory muscles. For example, the average person uses between one to two percent of his oxygen consumption in the form of energy to power in the process of breathing. Due to various diseases and trauma, the consumption of oxygen required to support breathing alone can approach, and even exceed, the ability of the lungs to provide it. This, of course, is where respirators come into use. Several articles provide a much more detailed discussion of the concept of the cost of breathing [19-21, 35].

What factors effect this cost of breathing? These factors are sufficiently lengthy and complex to provide the index of a good respiratory physiology textbook. With regard to the EVCS, the most conspicuous factor is the frequency of breathing. Mead [45] has suggested that there are two "optimal" frequencies determined by the body — one to minimize energy expenditure in the resting state and another to maximize gas exchange during exercise. These frequencies could be the result of the EVCS trying to optimize breathing for the particular situation. Other factors such as pain and voluntary control mediate the frequency. However, Ruttimann and Yamamoto [46] recently have shown mathematically that there are no unique frequencies for nonresting man using a simple pulmonary mechanics model. The other more conspicuous factor is depth of breathing or tidal volume. This is a function of the flow rate of air in the airways and the frequency of breathing resulting from the inverse of the sum of the time of inspiration and the time of expiration. It

is the result of much less conspicuous interactive factors, namely deadspace and airway mechanics.

The most obvious portion of the deadspace is called the mechanical deadspace which comprises the larger conductive bronchi, larynx and pharynx. The rest of the deadspace, part of whose volume is controllable by the EVCS, is called the physiologic deadspace. One part of this physiologic deadspace is controlled by the circulation of blood within the lungs. If air enters an alveolus with little or no perfusion, no gas can be exchanged, hence deadspace. Similarly, another portion of the physiologic deadspace is comprised of well-perfused alveoli with little air flow. Finally, there also are alveoli both poorly perfused and poorly ventilated. The EVCS, for purposes of this discussion, can control the pulmonary circulation [47], to allow more blood flow to better ventilated regions of the lungs. There are many references further describing coordination of ventilation and perfusion in detail [47-49]. The frequency of breathing [43] and the position of the person [51] effect the distribution of the air within the lungs.

The instantaneous pressure of the air as measured at the alveolus has a considerable effect on the deadspace. If the pressure/volume characteristic of the alveolus is examined, one sees that little pressure is required to fully inflate the alveolus, but a large pressure drop is required to deflate a fully inflated alveolus. An excellent discussion of the physical theory of this hysteresis phenomena is presented by Crane [52]. The specific shape and width of the hysteresis curve are determined by a substance called surfactant, which minimizes the surface tension thereby allowing the alveolus to be inflated with a minimum of

muscular effort [53-55]. The deflation of the alveolus is called atelectasis [56]. The EVCS has mechanisms such as bronchoconstriction [59, 60] to control alveolar pressure, hence controlling gas exchange by taking alveoli into or out of the pulmonary air circulation. This is accomplished by decreasing the alveolar pressure to deflate the alveolus or increasing it to inflate the alveolus.

The pulmonary mechanics observed at the mouth are the result of the interaction of 300 million alveoli with the external environment. The measurement of these mechanics and the instantaneous gas concentrations are helpful in examining the function of the EVCS. Yamashiro and Grodins [61] provide an excellent discussion of operational characteristics of the EVCS to minimize the expenditure of energy in breathing.

If we consider the integral of the product of the pressure and flow waveforms at the mouth over one breath, the work of breathing is obtained. It consists of two components as would be suggested by the airway model discussed earlier in conjunction with respirators (Fig. 1). The first is the resistive work causing the expenditure of energy in the form of muscle motion to inflate the lungs. The remainder of the work does not require the expenditure of the body's energy. This is the elastic energy exerted by the alveoli and rib cage used to deflate the lungs [2, 3]. The flow and pressure waveforms are controlled by the EVCS to minimize energy by the body in the breathing process. Once the frequency of respiration is set, the ratio of inspiratory time to expiratory time can be adjusted by the EVCS to help minimize the resistive work. Widdicombe and Nadel [62] have further proposed that the airway resistance be regulated in an optimal manner.

Finally, the total respiratory control system has been modeled by Yamamoto and Raub [27] and Yamashiro [21] with some success. Unfortunately, not all the components of the respiratory control system are known. Until they are, such studies as those on the stability of the respiratory control system [63, 64] are a bit premature. As one cybernetician put it, "there are few bugs in the respiratory control system that two billion years of research and development haven't solved [65]". However, the application of increasingly more sophisticated engineering and mathematical methods is aiding the continued refinement of respiratory control models. Examples of the more basic empirical techniques include sinusoidally varying the concentration of the inspired gases [69-71] and pressure [72] to obtain equivalent impedances for the models. Least squares estimation [66] and other statistical techniques [67, 68] exemplify the more sophisticated approaches of model identification techniques. All of these techniques, in conjunction with improved physiological transducers, will continue to improve the generality of respiratory control models.

1.2.3 Automated respirator control

A surprising amount of work has been done on automated respirator control. The first group of papers deals with servo control of inspired gas concentrations. Bellville, Fleischli and Attura [75] developed a servo control to instantaneously vary the concentration of inspired CO_2 in a sinusoidal manner. Earlier, Lambertsen and Wendel [76] used the measurement of the end expiratory CO_2 to control the inspired gas concentration. Pierce [73] developed a closed circuit system which

measures the oxygen consumption and removes carbon dioxide and supplies oxygen to maintain the desired gas concentrations within the closed system. Folgering et al. [74] have refined this type of closed circuit system even further.

The use of IPP ventilators can cause some harmful effects. Due to their wide spread use, there has been some work in minimizing these. Primarily, the effects are reduction of cardiac output [14, 15] and changes in the mechanical properties of the alveoli [57], as a result of controlling airway pressure and flow waveforms. Wald, Murphy and Mazzia [9] have done a theoretical study of controlled ventilation using the simple model of Fig. 1 (also Ruttimann and Yamamoto [46]). Different inspiratory flow waveforms such as rectangular, sinusoidal, exponential, positive ramp, and negative ramp were used to minimize the average alveolar pressure for a particular deadspace and alveolar ventilation. This minimization determines the optimal tidal volume and respiration rate. Jain and Guha [6, 78] have carried this even further by developing a control system to maintain a specific alveolar pressure.

Introducing air into the alveoli by proper consideration of airway mechanics is only half of the function of a respiratory; the introduced air must have an appropriate gas composition. An experimental system for maintaining a constant alveolar Pco_2 while experimentally changing the Po_2 was constructed by Holloman, Milhorn and Coleman [79]. It utilized the end expiratory Pco_2 to regulate the concentration of inspired gas to maintain a constant P_Aco_2. In 1969, Hilberman, Schill and Peters [80] outlined, by means of flowcharts and functional schematics, a respirator

control system to maintain a preset arterial Pco_2 through use of a sampled-data regulator. It considered the problem of the maintenance of the patient's cooperation (not fighting the respirator, a common behavior) by shutting off the patient's proprioceptive mechanisms for breathing through regulation of the P_Aco_2 as interpolated from the end expiratory Pco_2. It was an adaptive controller changing the ventilation in response to the patient's needs. The ventilation provided was bounded by the physician through limiting the parameters used to calculate the alveolar ventilation in Eq. (1-1) (namely the tidal volume, respiration rate and the mechanical portion of the deadspace). In 1971, Mitamura et al. [81] devised an "optimally" controlled respirator which controlled ventilation by measurement of the carbon dioxide output. It used a linearly estimated deadspace to estimate alveolar ventilation and varied the respiratory rate to minimize ventilatory work.

An optimally controlled respirator requires an adaptive controller. It must be able to determine and even anticipate the patient's needs for ventilation and provide for them. Since many of the parameters are unobservable on a continuous basis, the controller must blend clinical experience and theoretical knowledge. This dissertation will develop the physiological model for a respirator control utilizing the parameters measurable at the patient's mouth with emphasis on gas exchange parameters (Fig. 4). These parameters will be used by the controller to refine the physician-estimated respiratory control settings to provide a more accurate and prompt estimate of the patient's physiological needs for respiratory gas exchange. In Chapter 2, a model for the control system will be developed. In Chapter 3, the optimal control gas exchange

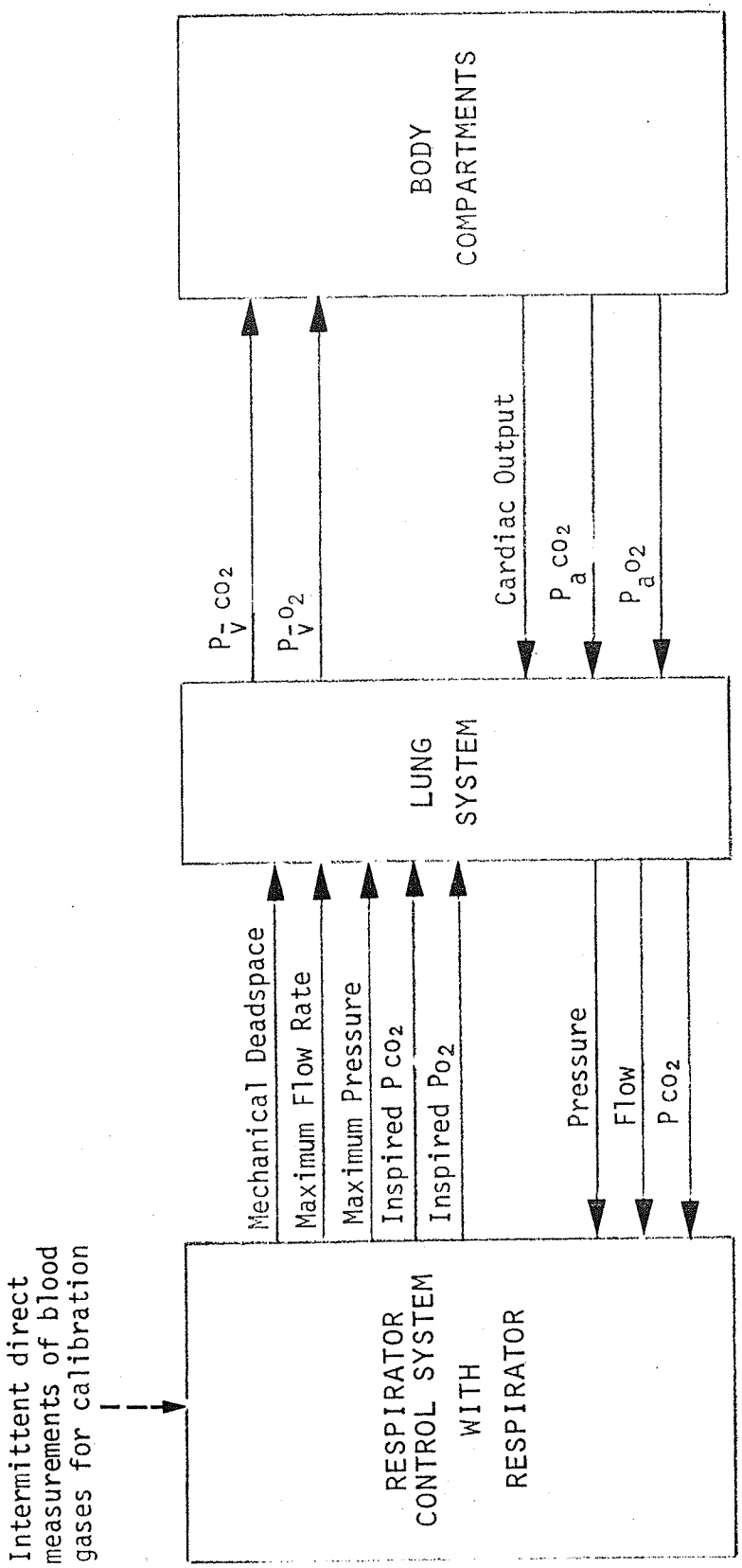

Figure 4. Measurable parameters of human respiratory system/respirator system.

will be discussed and a suboptimal set of control laws developed for the implementation. A summary of results and directions for future development will be discussed in Chapter 4.

2.4 Measurable Parameters of Respiration

To control ventilation extracorporally, it is necessary to obtain a measure of the body's response to the delivered ventilation. Pulmonary function testing which is usually used for patients not on respirators is well described elsewhere [101, 102]. Hence, this discussion will be limited to the parameters which are measurable at the patient's mouth and whose measurement does not require the change of the inspired gas concentrations (such as nitrogen washout techniques, and the like).

At the mouth there are four waveforms which provide useful information about the gas exchange occurring within the patient's lungs. The pressure and flow waveforms yield information about the pulmonary mechanics or the mechanical efficiency of the gas exchange and measure of particular gas volumes such as tidal, expiratory and deadspace. The oxygen and carbon dioxide concentration waveforms provide quantitative information about the gas exchange and are the basis for estimates of the gas concentrations in the blood. These four waveforms are illustrated in Fig. 10.

The pressure waveform is measured by inserting a pressure transducer into the airway at the mouth of the patient. A more accurate measurement of the pressure waveform for calculation of pulmonary mechanics is performed by placing a small (1 cc) balloon transnasally into the patient's esophagus. The balloon is then connected to a pressure transducer located outside of the patient by a thin, but firm, tube [103]. Unfortunately, this more accurate method is not tolerated very well by the patient both medically and emotionally.

The flow waveform's measurement is more complex since it is nonlinear due to turbulance. However, if several parallel plates are horizontally

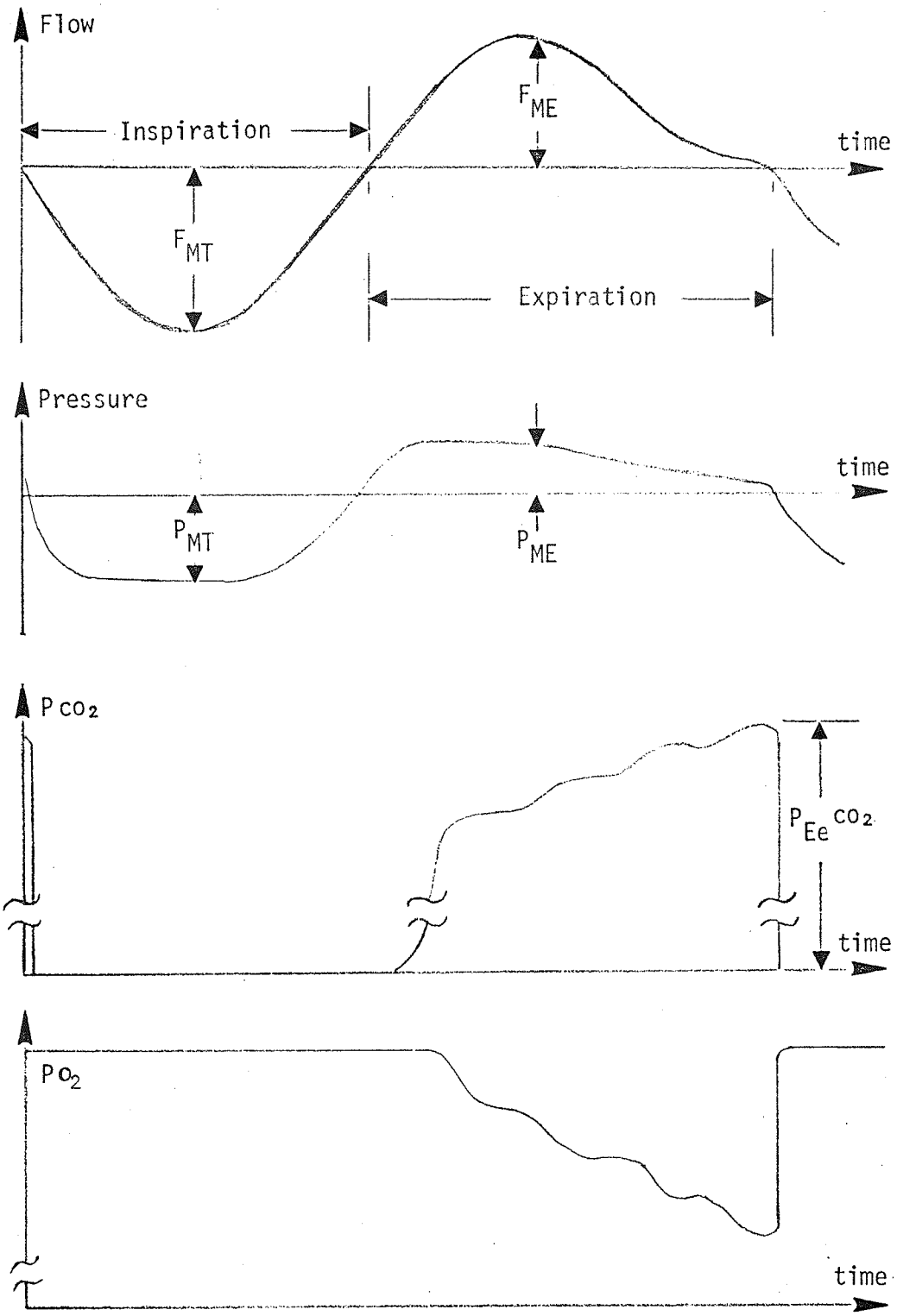

Figure 10. Respiratory waveforms measurable at the mouth.

inserted into air flow, the turbulance is eliminated and the flow becomes linear causing the differential pressure across the length of the plates to be linearly related to the airway flow. This is the principle of the pneumotachograph, which is most commonly used in practice. In clinical use, due to moisture accumulation problems, the prolonged continuous use of a pneumotachograph causes a decrease in accuracy. Elaborate systems have been developed to eliminate this problem. One system uses warm dry air added to the air flow in small quantities to flush the accumulated moisture out of the pneumotachograph [106]. In addition to moisture accumulation problems, the user must be aware of the limitations of their range of amplitude linearity and frequency response [104, 105]. A new promising flow meter uses ultrasound to create a doppler shift for air flow [105, 107]. It has the advantage that there is no heating source to prevent moisture condensation. Finally, a wire mesh flow meter has been developed [108]. The air flow cools a heated wire grid; the cooling is a measure of the amount of air flow.

The real-time measurement of the waveforms of the concentrations of the respiratory gases must use the spectrographic properties or rapid chemical reactions of these gases, since no other presently available method provides a sufficiently prompt response time to measure the rapid concentration changes that occur in these gases (Fig. 10). One commonly used device, Goddard Capnograph, uses the infra-red spectrum to determine the carbon dioxide concentration. It is fairly accurate (0.1% CO_2) and has a response time less than a tenth of a second. There are several sources of error in measurement. The first is the interference from

the overlapping of adjacent spectral peaks of other gases. This is resolved by chromatic filtering. Spectrum broadening due to the inelastic collision between the carbon dioxide molecules and those of other gases is another. However, since this phenomena is directly related to the concentration of the carbon dioxide, its effect can be eliminated by a linear correction factor. The capnograph tends to have a nonlinear response over a large range of carbon dioxide concentrations, but, in the present application, only a relatively narrow range of response will be needed.

A common oxygen measurement device is the Westinghouse oxymeter. Its operation is based upon the permeability of zirconium oxide to oxygen ions at high temperatures. The Po_2 differences between the respiratory gas and the external atmosphere cause a voltage difference to develop between the plates exposed to each of the two respective gas mixtures. This voltage is related to the Po_2 difference by the Nernst equation [110]. The physical structure of the oxymeter is a fuel cell whose external and internal platinum surfaces are coated with zirconium oxide. The oxymeter has a relatively fast response time (0.03-0.05 seconds). Unfortunately, the cells age rather rapidly, and, due to the high operating temperature of the fuel cell (about 960° C), it is an explosive hazard as well as having a source of error introduced by temperature related oxygen combustion.

The mass spectrometer combines the functions of both the capnograph and the oxymeter as well as the ability to determine the concentrations of several other gases such as nitrogen. Due to its high cost, it is used more in clinical research rather than normal patient care. However,

it is included here for completeness. The mass spectrometer is used to measure the fraction of the respiratory gases, not the partial pressure. Hence, some calibration and calculation are required. Water vapor present in the expired gases must be included in these calculations. Fortunately, it can be calibrated about specific values of the estimated fractional concentrations of the gases to provide both sensitivity and accuracy over a range of common physiological values. Detailed discussions of its operation and a more complete error analysis are treated elsewhere [110, 111]. There are other discussions of its use in a monitoring environment [113-115].

Although the respirator control is constrained to use only non-invasive techniques in estimating the alveolar, arterial and venous gas concentrations, several invasive direct techniques for the blood gas concentrations are noteworthy. Mass spectrometry has been used to make these measurements [113, 114] in quite the same manner as the respiratory gases were measured. Electrode systems have been developed to measure the pH and temperature, in addition to the gas concentrations in flowing blood [116]. Finally, the use of fiber optics to transmit light of two colors from the source to a sensor through blood has made it possible to directly measure the hemoglobin saturation (of oxygen) by use of the fact that the hemoglobin saturation is directly related to the color of the blood [117, 118].

From the four waveforms, many possible measurements are obtainable. This discussion will involve only a few of these. Turney, McAslan, Crawford and Adams [119] present a good compendium of the possible measurements. For the purposes of a respirator control system, the respiratory parameters

needed are the resistance, r, the compliance, c, tidal volume and expiratory volume, minute ventilation, total work, resistive work, mean and end expiratory Pco_2 and the end expiratory pressure. Note that the parameters of the oxygen waveform have been ignored in the prototype controller, although they will be used in later versions.

As was stated earlier, from a pneumatic standpoint, the lung can be represented by a simple series RC equivalent circuit. The resistance and compliance are estimates of this equivalent circuit. Their specific and relative values give the physician a good estimate of the gas exchange and the effort of the patient to maintain it. Since these values are only estimates, there are many methods for their determination [119-123, 126]. Since a computer is not available, some measurements are not possible. However, due to recent advances in integrated circuit technology, most measurements can be accommodated using a microprocessor and some analog preprocessing circuitry for each control system. Turney et al. [115] even uses a modified desk calculator to monitor a 12-bed respiratory word.

From the flow waveform, the tidal volume and expired volume can be obtained by simply integrating over the appropriate periods. Inspiration can be defined as the period which the air flows into the patient. By convention, its start is indicated by a negative zero crossing of the flow waveform, its end by a positive zero crossing. The occurrence of the negative zero crossing is used to trigger a sampling of the pressure waveform to obtain the end expiratory pressure, P_{Ee}, while the positive zero crossing is used for the end inspiratory pressure, P_{Ie}. The compliance is defined as the ratio of the tidal volume to the difference between the end expiratory and end inspiratory pressures.

The expired volume is calculated by integrating the flow waveform between the positive and negative zero crossings of the flow waveform. Since the tidal and expired volumes of the previous breath are known and since the patient on a respirator breathes relative constant volumes, the value of half of these volumes is also known. Hence, the flow and pressure waveforms can be sampled when the integral of the flow waveform is equal to half of the tidal and half of the expired volumes to obtain the midtidal flow and pressure, F_{MT} and P_{MT}, and the midexpiratory flow and pressure, F_{ME} and P_{ME}, respectively. These are used to calculate the Cook resistance [122] by dividing difference between midtidal and midexpiratory flows by the difference between the midtidal and midexpiratory pressures.

When the product of the instantaneous pressure and flow is measured, the instantaneous power is obtained. If the instantaneous power waveform is integrated over the total respiratory cycle, the resistive work is obtained. If it is only integrated over the inspiratory portion of the respiratory cycle, the total work is calculated. The resistive work indicates the amount of work lost (energy expended) during one breath while the total work is the amount of work used during a breath. The total work is greater than the resistive work since some of the work used for expansion of the chest during inspiration is stored in the form of potential energy stored in the elastic rib cage and alveoli. This potential energy and hence its related work is recovered during expiration. The difference between the total and resistive work is the work expended during inspiration, but which is recovered during expiration. This work is used to expand the chest, alveoli, and diaphragm. Since these have elastic properties, most of the energy spent inflating them is recovered during deflation. Other normalized measures of work or commonly used such as work per liter , work per breath divided by the tidal volume, and work per minute, the product of the work per breath and the respiration rate.

2.5 Measurable Respiratory Parameters and Respiratory Function

The values of respiratory parameters have significance in both their absolute value and their value relative to past history and particular pathology. "Emergency" indicants of problems with the mechanical and functional aspects of the control system use the absolute value of these parameters. For example, a sudden decrease from the nominal respiratory controller settings of the tidal volume and inspiratory pressure as measured at the patient's mouth would indicate a leak in the respirator's seals or tubing [128]. Similarly, a sudden decrease in expired volume would indicate the disconnection of the patient from the respirator. "Trends" usually occur over the period of several hours usually with only slight incremental relative changes observed over several sampling intervals.

From a different perspective, the measured parameters may have different meanings, which depend upon whether or not the patient has been stabilized. During the initial phase of the control when the patient has just been placed on the respirator, some of the parameters may vary over a wide range of values. The most obvious is the Pco_2 which is expected to change in order to reach the desired value, the major purpose of the controller as outlined in this dissertation. Less obvious is a change in the compliance, resulting from the increased number of alveoli participating in gas exchange. This is due to the respirator's positive inflationary pressure opening them up. Once a patient has achieved the desired Pco_2, i.e., respiration is stabilized, the parameter values usually also stabilize causing parametric values to be interpreted as trends.

Table 2 briefly describes the significance of several of the measurable respiratory parameters in regard to alarm and trend indications. For alarm indicants, direct measures of the characteristics of the input waveforms (flow, pressure and Pco_2) yield the best information. Although the derived parameters also reflect the existence of alarm conditions, this can be used by more sophisticated control conditions to determine the specific cause of the alarm condition. The pressure and flow waveform characteristics inform the control system of problems with delivery of the set ventilation, not only the amount of inspired air, but also the efficacy of the inspiration-expiration ratio (i.e., does the patient have sufficient time to expire the previously inspired volume of air?).

For gas exchange, the adequacy-of-oxygenation assumption eliminates the direct need to estimate the oxygen consumption from the O_2 waveform. However, a more comprehensive respirator control and pulmonary function evaluator can use this parameter. With regard to carbon dioxide, the end-expiratory Pco_2 is used as an estimate of the arterial Pco_2. In normal clinical practice [11], blood gas measurements are made every six to twelve hours after a patient's Pco_2 levels have stabilized due to proper ventilation. More frequent measurements are made when the patient is started on the respirator. The difference between the measured arterial Pco_2 from the blood gases and the measured end-expiratory Pco_2 from the control system is then used to recalibrate the control system's estimation of the arterial Pco_2 which it used for the basis of its regulation function.

Since the Radford nomograph estimates the ventilation required based on an estimation of the $\dot{V}co_2$, the respirator control system can use its measured $\dot{V}co_2$ to refine the ventilatory requirements on an empirical basis.

TABLE 2

THE SIGNIFICANCE OF SELECTED MEASURABLE RESPIRATORY PARAMETERS

	Alarm Indicator		Trend Indicator	
Parameter	Initial	Stabilized	Initial	Stabilized
F_{MAX}	yes	yes	no	no
P_{Ie}	yes	yes	no	no
P_{MT}	yes	yes	no	no
P_{Ee}	yes	yes	no	no
r	no	no	no	yes
c	no	no	no	yes
W_T	no	no	no	yes
W_R	no	no	no	yes
V_T	yes	yes	no	no
V_E	yes	yes	no	no
Vco_2	yes	yes	yes	yes
$P_{Ee}co_2$	no	no	yes	yes

The empirical measurement of $\dot{V}co_2$ has little meaning until the patient is stabilized at the desired Pco_2 level, since changes in gas storage as well as production are measured while the stabilization process is taking place. Once the patient is nearly stabilized, $\dot{V}co_2$ can be used to refine the ventilation to maintain an equilibrium about the desired Pco_2 level.

This discussion has been intentionally of a qualitative nature. The particular amount of change in the parameters used for the control system are of a patient-specific nature. In addition, clinical experience guides the determination of what percentage change in each parameter constitutes a trend condition.

2.6 Summary

To conclude the discussion of the physiologic basis of a respirator control system, let us integrate the concepts already discussed. First, our purpose is to design a control system to provide the proper ventilation for the patient. Proper ventilation, as was pointed out earlier, maintains the blood gas levels within specific physiologically defined limits. Next, due to reasonable medical and economic constraints placed upon a respirator control system, these levels may be estimated from phenomena observable at the mouth, but the observer must beware. Both the patient's specific physiology and the dynamics of human gas exchange greatly effect the accurate estimation of the blood gas level. Nevertheless, after calibration, a system can accurately make these estimates to be used by the respirator control system to regulate ventilation.

Finally, the model discussed in this chapter is not intended to be a model applicable to all patients. There are many forms of respiratory failure, each with its own form of dysfunction. The model used here is based on an answer to the question: What can one determine about a patient's respiratory functioning using noninvasive techniques but knowing little about the specific pathology? The answer given by the model is applicable to a subset of all patients requiring respirator support. The definition of his subset will be determined clinically. The importance of this model lies in the fact that it can provide the basis for a respirator control system that will respond quickly to the patient's respiratory needs.

3. AUTOMATED CONTROL OF CARBON DIOXIDE EXCHANGE

This chapter deals with the mathematical definition of control problems using the model developed in Chapter 2. From these definitions, solutions will be obtained to define a regulator for the automated control of CO_2 gas exchange as a first step for a respirator control system. The motivation of the chapter is to investigate the various ways of formulating the control problem to find the easiest to implement. An automated respirator control system that requires a large scale computer cannot be justified from an economic basis. Therefore, a controller must be implementable by a relay system, analog, hybrid computer or microprocessor to be generally available to patients.

Section 3.1 will deal with the mathematical definition of the optimal control problem considering important physiological constraints. It will be shown that although the mathematical definitions of the system dynamics are nonlinear, a linearized definition will be adequate.

Section 3.2 will deal with the continuous control problem. It will consider both the time optimal and the quadratic performance indices and their results.

Realistically, the measurable parameters are not continuously observable, so Section 3.3 will deal with the sampled-data control problem. Again, the time optimal and the quadratic performance indices will be considered. Only a fixed interval sampling scheme will be considered.

The application of the Maximum Principle to the continuous time optimal problem will be considered in Section 3.4. The solution for the control function is really equivalent to a sampled-data time optimal control problem with variable sampling intervals.

3.1 Bilinear Control Systems and the Formulation of the Control Problem

Until the late 1960's, bilinear control systems as such were a relatively unresearched area. Usually approximate linear models were frequently used to describe the dynamic behavior of nature's nonlinear processes. The bilinear model of a nonlinear process is one step beyond the linear model since it has a linear term for both the state and control variables and a nonlinear term of the products of the state and control variables. Many natural nonlinear processes can be modeled using a set of bilinear dynamic equations. Mohler [130, with Smith, 131] has suggested that such biological processes as the population of a species, catalytic chemical reactions, compartmented physiological models and hemostatic regulators, such as respiratory, cardiac and thermal regulatory systems, are bilinear in form. In physical systems, bilinear systems appear in such complex dynamic systems as nuclear fusion processes and heat transfer to more mundane applications such as the braking system of automobiles.

In 1968, Rink and Mohler [132] first published the sufficient conditions for completely controllable bilinear systems. Later that same year, they presented a method of synthesis for bilinear control [133]. Moon [143] later showed that if the state variables are phase-related and linear in control, and if a time optimal control does exist, it is "bang-bang" in nature just as for linear systems. Due to algebraic complexities, most of the theory of bilinear control systems has been developed from geometric arguments.

Using a reduced model of the Farhi and Rahn type as shown in Fig. 10, let us define the control problem which is in bilinear form. Note that

the "slow" compartment has been ignored since it will little effect dynamic state equations. Similarly, the capacitance of alveolar compartment has been ignored (indicated by the dotted capacitor) and has been replaced by a capacitance representing the CO_2 storage in the blood. In Fig. 11, the voltages (corresponding to Pco_2) across each capacitor are defined as the state variables. The reciprocal of the resistance in the alveolar compartment is defined as the control variable v. Note that ignoring the alveolar capacitance has an effect on the specific value of v, but the ignored resistance can be incorporated later as an additive term to the value of v (note v is also referred to as the ventilation).

The dynamic state equations are:

$$\dot{y}_1 = -a_{12}y_1 - b_1y_1v + a_{12}y_2 \tag{3-1a}$$

$$\dot{y}_2 = a_{21}y_1 - a_{21}y_2 + c_2' \tag{3-1b}$$

where

$$a_{12} = \frac{1}{c_1r_2} \tag{3-2a}$$

$$a_{21} = \frac{1}{c_2r_2} \tag{3-2b}$$

$$b_1 = \frac{\alpha}{c_1} \tag{3-2c}$$

$$c_2' = \frac{I_2}{c_2} = \frac{\dot{V}co_2}{c_2} \quad . \tag{3-2d}$$

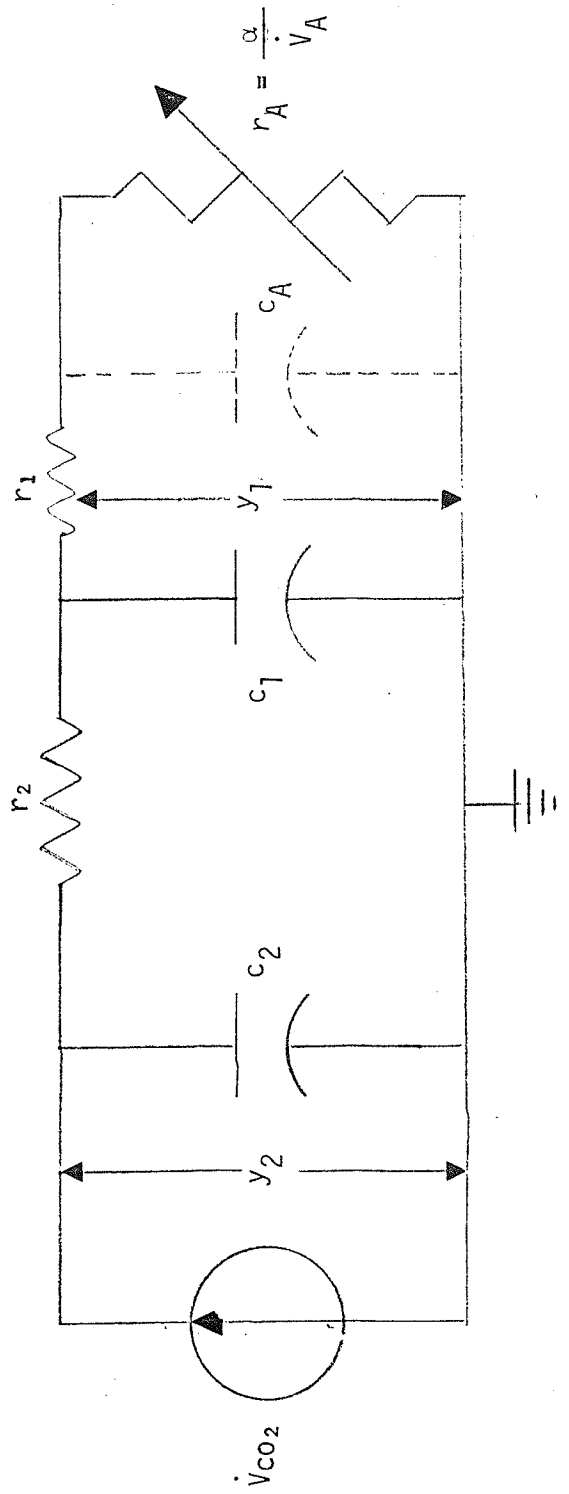

Figure 11. The reduced physiological model for gas exchange.

The control variable, v, must be constrained by the following relationship:

$$0 < v_{min} \leq v \leq v_{max} \tag{3-3}$$

and, for physical reasons, the state variables must be constrained

$$0 < \underline{y} \quad . \tag{3-4}$$

Since we desire to have the control necessary to transfer the system from an initial state, $\underline{y}_0$, to a final equation state, $\underline{y}_f$, in a minimum time, the cost function used in this analysis is:

$$J = \int_{t_0}^{t_f} dt \quad . \tag{3-5}$$

However, the time optimal solution may not be ideal from a patient's perspective, so an error-nulling or quadratic-performance index will also be considered:

$$J = \int_{t_0}^{t_f} (\underline{y} - \underline{y}_e)^T Q(\underline{y} - \underline{y}_e) + rv^2 \, dt \tag{3-6}$$

where $\underline{y}^T$ is the transpose of $\underline{y}$.

Directly applying the Maximum Principle of Pontryagin [118] to the differential equations of Eq. (3-1) and the cost functional of Eq. (3-5), we obtain a "bang-bang" type of solution of the control — sequence of alternate application of v_{max} and v_{min} to reach the final state of $\underline{y}_f$. Physically, this means alternate extreme hyperventilation and extreme hypoventilation which is not well tolerated by the patient. Also, the

equilibrium ventilation, v_e, (causing $\dot{\underline{y}} = 0$) must lie within the prescribed bounds of Eq. (3-3) for a final equilibrium state to be possible. Finally, it has been suggested that too rapid a change of the Pco_2 causes cardiac rhythmias [128] and other undesireable side effects [11]. Since the state variables either are barely physically observable or are mathematical constructs, measurements of their rates of change or placing constraints on their rates of change in the formulation of the problem compounds the difficulty of observation and of solution of the control problem. Instead, let us place a constraint on the rate of change of the control variable v.

Let us define a new state variable

$$y_3 = v \tag{3-7}$$

under the same constraint of Eq. (3-3) and a new dynamic equation

$$\dot{y}_3 = u = \dot{v} \tag{3-8}$$

where

$$|u| \leq \eta < \infty \quad . \tag{3-9}$$

The addition of the new state variable has two effects. First, this constraint allows medically reasonable changes in the Pco_2 to occur for the proper initial v, (v_0) and the bounds of the rate of change of v. Secondly, the "bang-bang" type of ventilation is eliminated.

To reformulate the control problem to make use of the additional state variable and to eliminate unnecessary constants, let us define the equilibrium state $\underline{y}_e$, where $\dot{\underline{y}} = \underline{0}$ by

$$\underline{y}_e = \begin{bmatrix} y_{1e} \\ y_{1e} + \dot{V}co_2 r_2 \\ \dfrac{\alpha \dot{V}co_2}{y_{1e}} \end{bmatrix} \tag{3-10}$$

for a specifically chosen y_{1e}, the $P_a co_2$. Using this, let us make the following transformation:

$$\underline{x} = \underline{y} - \underline{y}_e \tag{3-11}$$

to obtain our new dynamic equations

$$\dot{x}_1 = -(a_{12} + b_1 y_{3e})\, x_1 + a_{12} x_2 - b_1 x_1 x_3 - b_1 y_{1e} x_3 \tag{3-12a}$$

$$\dot{x}_2 = a_{21} x_1 - a_{21} x_2 \tag{3-12b}$$

$$\dot{x}_3 = u \tag{3-12c}$$

under the new end conditions

$$\underline{x}_0 = \underline{y}_0 - \underline{y}_e \tag{3-13a}$$

and

$$\underline{x}_f = 0 \tag{3-13b}$$

assume that $\underline{y}_e$ is the desired equilibrium.

If the eigenvalues of the autonomous system (zero value of control variable) described by Eq. (3-12) are calculated, then it is indicated

that the slow one remains relatively constant over a wide range of ventilation (x_3) in Table 3. The fast eigenvalue does vary more markedly over the range of ventilation. However, since fast mode is on the order of seconds when we are looking at the model in terms of variations over several minutes, its effect can be ignored. This result is valid for variations of the model parameters of ±50 percent. Therefore, a model linearized with respect to ventilation, x_3, is valid over the range to be considered.

TABLE 3

EIGENVALUES OF AUTONOMOUS NONLINEAR EQUATION

x_3	Eigenvalue 1	Eigenvalue 2
-4000.	-0.372673E 01	-0.841323E-02
-3000.	-0.380116E 01	-0.123727E-01
-2000.	-0.387574E 01	-0.161796E-01
-1000.	-0.395046E 01	-0.198419E-01
0.	-0.402532E 01	-0.233675E-01
1000.	-0.410031E 01	-0.267635E-01
2000.	-0.417542E 01	-0.300366E-01
3000.	-0.425865E 01	-0.331932E-01
4000.	-0.432599E 01	-0.362390E-01
5000.	-0.440143E 01	-0.391796E-01
6000.	-0.447697E 01	-0.420202E-01
(ventilation)	(fast mode)	(slow mode)

For c_1 = 0.148E 02, c_2 = 0.250E 03, r_2 = 0.200E-01

3.2 Linearized Continuous Problem

This section deals with the linearized continuous formulation of the optimization problem. [By linearized, it is meant that we are ignoring the x_3x_1 term of Eq. (3-12a).] Both time and quadratic performance index criteria will be considered. Note that although the state variables may not be observable continuously, these formulations may provide insight to a simpler suboptimal solution.

3.2.1 Linearized time optimal continuous

Let us consider the linearized problem using the system described by the vector differential Eq. (3-12)

$$\dot{\underline{x}} = A_{3L}\underline{x} + B_{3L}u \quad . \tag{3-14}$$

The time-optimal cost functional is

$$J = \int_{t_0}^{t_f} dt$$

and the initial state $\underline{x}(t_0) = \underline{x}_0$ and the final state $\underline{x}(t_f) = \underline{0}$. The controllability matrix G of the above system is given by

$$G = [B_{3L} : A_{3L}B_{3L} : A_{3L}^2 B_{3L}]$$

$$G = \begin{bmatrix} 0 & -b_1 y_{1e} \eta & (a_{12} + b_1 y_{3e})\, \eta b_1 y_{1e} \\ 0 & 0 & -a_{21} \eta y_{1e} \\ \eta & 0 & 0 \end{bmatrix} \quad . \tag{3-15}$$

By inspection, G is nonsingular and the determinant of G is nonzero; therefore, the system is controllable and normal [136].

The characteristic equation of this system is

$$\Phi_c(s) = \sum_{i=0}^{3} \alpha_i s^i$$

$$= s^3 + (a_{21} + a_{12} + b_1 y_{3e})\, s^2 + b_1 y_{3e} a_{21} s = 0 \quad . \tag{3-16}$$

Using the values of α_i, let us define the matrix M such that

$$M = \begin{vmatrix} \alpha_1 & \alpha_2 & \alpha_3 \\ \alpha_2 & \alpha_3 & 0 \\ \alpha_3 & 0 & 0 \end{vmatrix} \quad . \tag{3-17}$$

Let λ_i be the roots of $\Phi_c(s)$ such that

$$\lambda_0 = 0 \tag{3-18a}$$

$$\lambda_1 = -b - \sqrt{b^2 - c} \tag{3-18b}$$

$$\lambda_2 = -b + \sqrt{b^2 - c} \tag{3-18c}$$

where

$$b = (a_{21} + a_{12} + b_1 y_{3e})/2$$

$$c = b_1 y_{3e} a_{21} \quad .$$

A transform can be applied to $\underline{x}$ such that the state equation becomes

$$\dot{\underline{x}}^* = A_{3c}\underline{x}^* + B_{3c}u \tag{3-19}$$

where

$$\underline{x}^* = GM\underline{x}$$

$$A_{3c} = [GM]^{-1} A_{3L} GM$$

$$B_{3c} = [GM]^{-1} B_{3L} \quad .$$

The form of $\underline{x}^*$ is called the phase variable canonical form.

Let us define a new transformation, T, such that

$$T = \begin{vmatrix} 1 & 0 & 0 \\ -\lambda_1 & 1 & 0 \\ \lambda_1\lambda_2 & -(\lambda_1 + \lambda_2) & 1 \end{vmatrix} \quad . \tag{3-20}$$

Another system whose control law has been well defined by Ryan [138] is defined as

$$\dot{\underline{v}} = A_{3v}\underline{v} + B_{3v}u \tag{3-21}$$

where

$$\underline{v} = TGM\underline{x}$$

$$A_{3v} = [TGM]^{-1} A_{3L} TGM$$

$$B_{3v} = [TGM]^{-1} B_{3L}$$

Since this system is linear of third order and has the real eigenvalues of the A_{3L} matrix ordered such that

$$\lambda_1 < \lambda_2 < 0 \tag{3-22}$$

the control law is as follows:

$$u = \begin{cases} -\text{sgn}[\phi(\underline{v})] & \text{for } \phi(\underline{v}) \neq 0 \\ -\text{sgn}[\sigma(\underline{v})] & \text{for } \phi(\underline{v}) = 0 \end{cases} \tag{3-23}$$

where

$$\phi(\underline{v}) = v_1 + \frac{v_2}{\lambda_1 - \lambda_2} + \frac{v_3}{\lambda_1(\lambda_1 - \lambda_2)}$$

$$+ \frac{\text{sgn}(\sigma)}{a\lambda_1^2(\lambda_1 - \lambda_2)} \left\{ \exp[-a\lambda_1 v_3 \text{sgn}(\sigma)]\, H_p(2 - H_p) - 1 \right\}$$

$$H_p = H^{\lambda_1/\lambda_2}$$

$$H = 1 + \sqrt{1 - [1 + G\ \text{sgn}(\sigma)]\ \exp[a\lambda_2 v_3 \text{sgn}(\sigma)]}$$

$$\sigma(\underline{v}) = \sigma = v_3 + \frac{\text{sgn}(G)}{a\lambda_3}(1 + |G|)$$

$$G = -a\lambda_2(\lambda_2 v_2 + v_3)$$

λ_1, λ_2 nonzero roots of the characteristic equation $\Phi_c(s) = 0$

sgn $(\cdot)$ = signum function $\triangleq \cdot/|\cdot|$

$|\cdot| \triangleq$ absolute value function

$a = 1/a_{21}$

$\underline{v}$ = the new coordinates $[v_1, v_2, v_3]^T$.

This control, when implemented, presents several problems. The first is the value of H_p. Since it is a number raised to the power of the ratio of λ_1 to λ_2 and the magnitude of that ratio is a large positive number, H_p is a large number. This causes overflows when calculated on the computer. Next, other products also cause overflows. Therefore, overflow protection is needed either in the control law program or by the computers system software. Since the sign of the product of these large numbers is used, such a computational adjustment will not effect the validity of the control calculated. Negative logrithmic protection is needed due to accumulated computational errors. Additionally, negative square root calculation protection is needed. The examples given by Ryan have eigenvalues of similar magnitude; therefore, his control law works nicely. The control law program is presented in Appendix B.

The switching manifold in three space turns out to be nearly coplanar with the x_1 - x_2 plane shown as in Fig. 12. This means that the system response is sufficiently fast that a switching in control is only needed as the origin (or the x_1 - x_2 plane) is approached from nonzero values of x_3. Within reasonable physiological values related to $\underline{x}$, the switching plane is really a plane and not some other form of a manifold. Therefore, although computationally difficult, this control law seems to be implementable in an approximate form in a relatively simple manner.

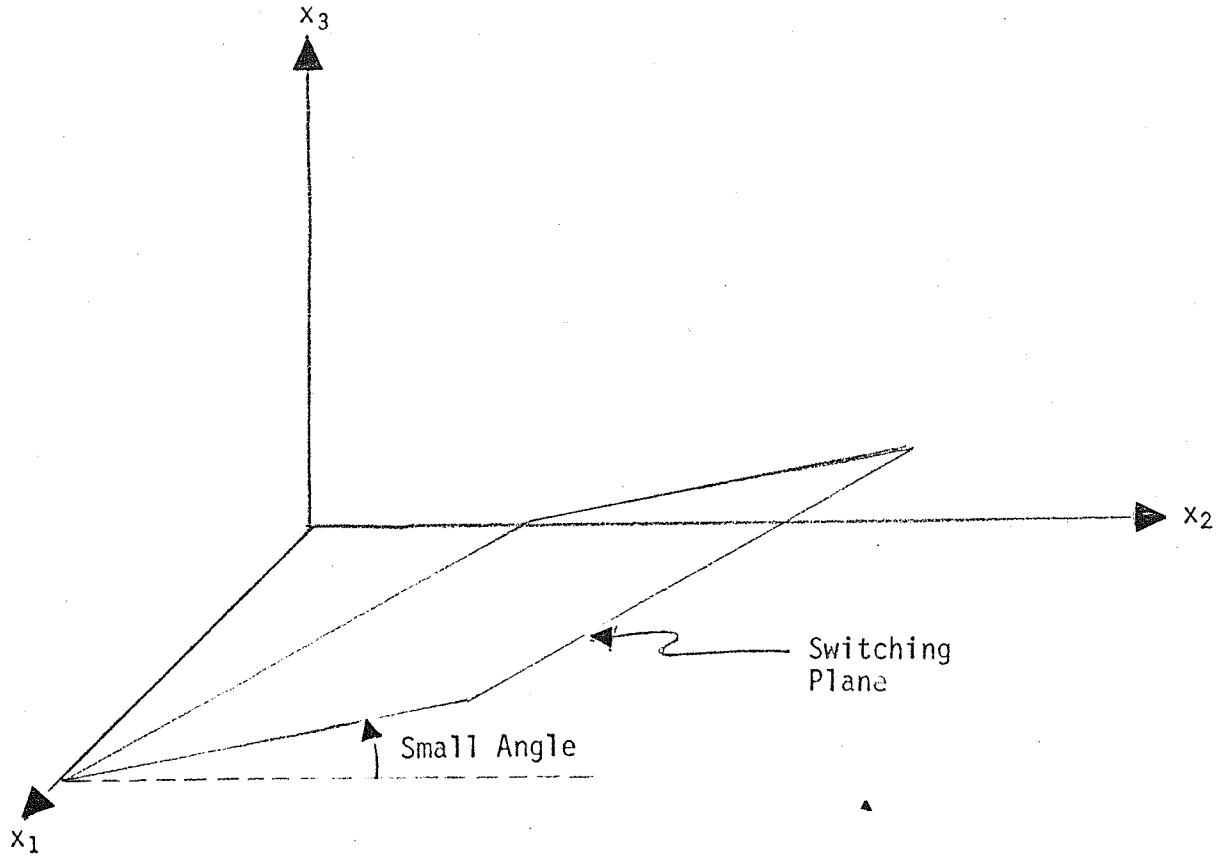

Figure 12. Time optimal switching plane.

3.2.2 Linearized continuous quadratic performance index

Let us reconsider the problem using the same linearized system but changing the performance index to

$$J = \int_{t_0}^{t_f} \underline{x}^T Q \underline{x} + ru^2 dt \tag{3-24}$$

where Q is a positive definite symmetric matrix, and r is a scalar greater than zero. The system is driven from the initial state $\underline{x}(t_0) = x_0$ to the final state $\underline{x}(t_f) = \underline{0}$.

Then, there exists a unique control u that is a function of the state variables [137], i.e.,

$$u = -\frac{1}{r} B_{3L}^T K \underline{x} = H\underline{x} \tag{3-25}$$

where K is a positive definite symmetric matrix, which is the solution of the nonlinear matrix algebraic equation, the Ricatti equation,

$$-KA_{3L} - A_{3L}^T K + \frac{1}{r} KB_{3L} B_{3L}^T K - Q = \dot{K} \tag{3-26}$$

and where A^T is the transpose of the matrix A. If we allow t_f to be very large, $\dot{K}$ approaches zero. This allows a simpler computational solution.

With the control as a function of the state variables, the optimal solution to the state dynamics is homogeneous

$$\dot{\underline{x}}(t) = G\underline{x}(t) \tag{3-27}$$

where $G = A_{3L} - \frac{1}{r} B_{3L} B_{3L}^T K$.

Using the symmetry of K, we can form a vector k and that

$$k = [k_{11}, k_{12}, k_{13}, k_{22}, k_{23}, k_{33}]^T$$

where each k_{ij} represents the ith row and jth column of the K matrix. Using this new vector, the Ricatti equation can be written as

$$A_k \underline{k} + B_k = 0 \tag{3-28}$$

where

$$A_k = \begin{vmatrix} 2(a_{12} + b_1 y_{3e}) & -2a_{21} & 0 & 0 & 0 & 0 \\ -a_{21} & (a_{21} + a_{12} + b_1 y_{3e}) & 0 & -a_{21} & 0 & 0 \\ b_1 y_{3e} & (a_{12} + b_1 y_{3e}) & 0 & 0 & -a_{21} & 0 \\ 0 & -a_{12} & 0 & 2a_{12} & 0 & 0 \\ 0 & b_1 y_{3e} & -a_{12} & 0 & a_{21} & 0 \\ 0 & 0 & 2b_1 y_{3e} & 0 & 0 & 0 \end{vmatrix}$$

$$B_k = \begin{vmatrix} \frac{n}{r} k_{13}^2 - q_{11} \\ \frac{n}{r} k_{13} k_{23} - q_{12} \\ \frac{n}{r} k_{13} k_{33} - q_{13} \\ \frac{n}{r} k_{23}^2 - q_{22} \\ \frac{n}{r} k_{23} k_{33} - q_{23} \\ \frac{n}{r} k_{33}^2 - q_{33} \end{vmatrix}$$

and where q_{ij} is the ith row and jth column element of the Q matrix.

This vector equation is a set of six simultaneous nonlinear equations in six unknowns. A modified Newton/Rhapson approach was first used to solve these equations. However, due to their wide range in magnitude of the k_{ij}'s, convergence on a solution was not possible in a reasonable number of iterations. Scaling and self-scaling methods were considered [138]; however, the eigenvector method of Potter [139] was chosen for expediency (Appendix B).

The eigenvalues of the state feedback matrix, G, do not vary significantly with respect to the model parameters. However, they are sensitive to changes in the Q matrix, the maximum time rate of change of the ventilation allowable, η, and the carbon dioxide output, $\dot{V}co_2$ (Table 4).

No integration was performed using the feedback gains derived from the Ricatti equation. However, it would be safe to say that for large values of the elements of Q matrix, the solution would approach the final state faster than that of the time optimal solution. However, the rate of change of x_1 and x_2 for such a solution would exceed physiologically safe limits.

It is important to point out that the calculation of the Ricatti matrix involves a great deal of computation for a specific set of parameters. Whether or not the Newton/Rhapson method, some self-scaling method or the eigenvector method is used, six dimensional matrices are used in the calculations. The calculation of the inverse of such matrices or methods of directly avoiding its calculation such as L-U decomposition (Appendix B) or the calculation of eigenvectors require sufficient computation as to render them impractical for present microprocessor

TABLE 4

EIGENVALUE COMPARISON

Condition	Eigenvalue 1	Eigenvalue 2	Eigenvalue 3		
Quiescent	-2.50000E 02	-3.97957E 00	-2.12822E-02	#	standard point
Q1 DECR	-2.50000E 02	-3.97945E 00	-2.12251E-02	*	Q matrix sensitivity
Q1 INCR	-7.90569E 03	-3.97945E 00	-2.12251E-02	*	
Q1 Q2 IN	-2.50000E 02	-3.98068E 00	-2.23564E-02	*	
Q1 Q2 IN	-2.50000E 02	-3.99175E 00	-2.68168E-02	*	
Q1 Q2 Q3	-2.50000E 04	-3.97945E 00	-2.12251E-02	*	
Q1 Q2 Q3	-2.50000E 03	-3.97918E 00	-2.12004E-02	*	
C1 DECR	-2.50000E 02	-5.80365E 00	-2.15981E-02		c_1 sensitivity
C1 INCR	-2.50000E 02	-3.97957E 00	-2.12822E-02		
C2 DECR	-2.50000E 02	-4.09979E 00	-3.44303E-02		c_2 sensitivity
C2 INCR	-2.50000E 02	-3.94965E 00	-1.78696E-02		
R2 DECR	-2.50000E 02	-7.55677E 00	-2.24155E-02		r_2 sensitivity
R2 INCR	-2.50000E 02	-2.78786E 00	-2.02531-02		
ETA=500.	-5.00000E 02	-3.97957E 00	-2.12822E-02		η sensitivity
ETA=750.	-7.50000E 02	-3.97957E 00	-2.12822E-02		
VCO2 DEC	-2.50000E 02	-3.89901E 00	-1.74046E-02		$\dot{V}co_2$ sensitivity
VCO2 INC	-2.50000E 02	-4.06029E 00	-2.50098E-02		

* Change in Q Matrix in diagonal form where Qi corresponds to q_{ii}

Q1 = 1

Q1 = 1,000

Q1 = 1,000, Q2 = 1,000

Q1 = 1,000, Q2 = 10,000

Q1 = 10,000, Q2 = 10,000, Q3 = 10,000

Q1 = 1,000, Q2 = 100, Q3 = 100

Quiescent values c_1 = 14.8, c_2 = 250., r_2 = .02, Vco_2 = 250., η = 250, Q = 0 except for q_{11} = 100, q_{22} = 10, q_{33} = 1 and r^2 = 1

implementation because they induce a significant delay in the response of the control system. In addition, the number of significant figures necessary to avoid numeric rounding error propagation due to the repeated multiplications and divisions necessary is beyond the present state of the art of microprocessors.

3.3 Sampled-Data Problem

Prior to examining the sampled-data control problems, it is necessary to define continuous state equation in sampled-data formulation. For the linear continuous system,

$$\dot{\underline{x}} = A_{3L}\underline{x} + B_{3L}u \quad . \tag{3-29}$$

By applying the Laplace Transform theory, it can be shown that

$$\underline{x}(t) = \Phi(t)\underline{x}(0) + \int_{t_0}^{t} \Phi(t - \tau)B_{3L}u(\tau)d\tau \tag{3-30}$$

for $t > t_0$, where

$$\Phi(t) = \mathcal{L}^{-1}[sI - A_{3L})^{-1}]$$

$(\cdot)^{-1}$ = matrix inverse

$\mathcal{L}^{-1}[\cdot]$ = inverse Laplace operator.

Under the assumptions that $t_0 = kT$, $t = (k+1)T$ for a uniform sampling interval T, it can be easily shown that

$$\underline{x}[(k+1)T] = \Phi(T)\underline{x}(kT) + \Theta(T)m(kT) \tag{3-31}$$

which is the discrete state transition equation with

$$\Theta(T) = \int_{kT}^{(k+1)T} \Phi[(k+1)T - \tau]B_{3L}u(\tau)d\tau$$

and

$$u(\tau) = m(kT) \quad \text{for} \quad kT \leq \tau < (k+1)T \quad .$$

For our system, each element of the Φ and Θ matrices can be calculated.

For the Φ matrix,

$$\phi_{11}(t) = \frac{-C_{22}}{\lambda_2 - \lambda_1}\left[(1 + \frac{\lambda_1}{C_{22}}) \exp(-\lambda_1 t) - (1 + \frac{\lambda_2}{C_{22}}) \exp(-\lambda_2 t)\right]$$

$$\phi_{12}(t) = \frac{C_{12}[\exp(-\lambda_1 t) - \exp(-\lambda_2 t)]}{\lambda_2 - \lambda_1}$$

$$\phi_{13}(t) = \frac{C_{13}C_{22}}{\lambda_1\lambda_2}\left[1 + \frac{(1 + \frac{\lambda_1}{C_{22}})\lambda_2 \exp(-\lambda_1 t) - (1 + \frac{\lambda_2}{C_{22}})\lambda_1 \exp(-\lambda_2 t)}{\lambda_1 - \lambda_2}\right]$$

$$\phi_{21}(t) = \frac{C_{21}[\exp(-\lambda_1 t) - \exp(-\lambda_2 t)]}{\lambda_2 - \lambda_1}$$

$$\phi_{22}(t) = \frac{C_{11}}{\lambda_2 - \lambda_1}\left[(1 + \frac{\lambda_1}{C_{11}}) \exp(-\lambda_1 t) - (1 + \frac{\lambda_2}{C_{11}}) \exp(-\lambda_2 t)\right]$$

$$\phi_{23}(t) = \frac{C_{13}C_{21}}{\lambda_1\lambda_2}\left[1 + \frac{\lambda_2 \exp(-\lambda_1 t) - \lambda_1 \exp(-\lambda_2 t)}{\lambda_1 - \lambda_2}\right]$$

$$\phi_{31}(t) = 0$$

$$\phi_{32}(t) = 0$$

$$\phi_{33}(t) = 1 \quad .$$

Then the Θ matrix is given by

$$\theta_1(t) = \frac{-C_{13}C_{22}\eta}{\lambda_1\lambda_2}\left\{T + \frac{(1 + \frac{\lambda_1}{C_{22}})\lambda_2^2[1 - \exp(-\lambda_1 t)] - (1 + \frac{\lambda_1}{C_{22}})\lambda_1^2[1 - \exp(-\lambda_2 t)]}{\lambda_1\lambda_2(\lambda_1 - \lambda_2)}\right\}$$

$$\theta_2(t) = \frac{C_{13}C_{21}\eta}{\lambda_1\lambda_2}\left\{T + \frac{\lambda_2^2[1 - \exp(-\lambda_1 t)] - \lambda_1^2[1 - \exp(-\lambda_2 t)]}{\lambda_1\lambda_2(\lambda_1 - \lambda_2)}\right\}$$

$$\theta_3(t) = \eta T$$

where

$$C_{11} = -(a_{12} + b_1 y_{3e})$$

$$C_{12} = a_{12}$$

$$C_{13} = -b_1 y_{1e}$$

$$C_{21} = a_{21}$$

$$C_{22} = -a_{21} \quad .$$

There are several properties of the state transition matrix, $\Phi(t)$, that are important in validating the solution of the inverse Laplace transform in Eq. (3-30) and for use in the derivations later in this section. The first is that

$$\Phi(t=0) = I \quad \text{(the identity matrix)} \tag{3-32}$$

This means that at t = 0 all the diagonal elements of Φ are one and the off diagonal terms are zero. In the derivations later in this section, the following two properties will be utilized:

$$\Phi^{-1}(t) = \Phi(-t) \tag{3-33}$$

$$\underbrace{\Phi(T)\Phi(T)\ldots\Phi(T)}_{k} = \Phi^{k}(T) = \Phi(kT) \quad . \tag{3-34}$$

It is interesting to note that the sampled-data formulation of the ventilation state variable, x_3, is identical to that of the continuous time optimal formulation except that any change in u(t) occurs at only a multiple of the sampling period, T, instead of when the system crosses the continuous system switching manifold.

3.3.1 Sampled-data — time optimal problem

Given the sampled-data state equation, the formulation of the time optimal problem states that the system moves from a state $\underline{x}_0$ to a state $\underline{x}(t) = \underline{0}$, where t is a multiple of the sampling interval, T, and $|m(iT)| \leq 1$, $m(t) = m(iT)$ for $iT \leq t \leq (i+1)T$.

For a given number of sampling periods N and the final state $\underline{x}(NT) = \underline{0}$, a recursive relationship between the initial state and the control vector that defines the region of controllability is:

$$\underline{x}(0) = -\sum_{i=0}^{N-1} S_i m(iT) \tag{3-35}$$

where

N = number of sampling periods

$S_i = \Phi[(i-1)T]\Theta(T)$

m(iT) = the control at the ith sampling period

and where the set of m(iT), [m(iT), i = 1, N], includes all permutations of sequence m(iT) = ±1.

This region of controllability is defined in space by a polyhedron whose vertices represent one sequence of length N of values for m(iT), i = 0, ..., N - 1. For example, if N = 2, the vertices of the polygon π_2 are found from the following sequences of controls: [1, 1], [-1, 1], [1, -1], [-1, -1]. These sequences placed into Eq. (3-35) give each vertex of π_2. In our case, π_i is the closed 3-dimensional surface with planar faces between adjacent vertices (i > 1). π_1 is a line. Since $|m(iT)| \leq 1$, the trajectory from any vertex j of π_i is a unique optimal trajectory following the jth control sequence $[m_0, m_1, \ldots, m_{i-1}]$, where j is the jth permutation of $|m_k| = 1$, for k = 0, ..., i - 1. However, if the system is nth order, the control sequence $[m_0, m_1, \ldots, m_{N-1}]$ is uniquely determined with $N \leq n$. If N > n, there is a set of time optimum solutions.

As is evident from the previous discussion, the optimal control strategy is dependent upon the initial state of the system. Basic to the solution is determining which π_i contains $\underline{x}(0)$. This involves a great deal of digital computation and puts a severe limitation on the practical implementation. If the S_i's of Eq. (3-35) are placed in matrix

form, $[S_0 : S_1 : \cdots : S_{N-1}]$, and this matrix is invertable, the m_i can be expressed in terms of $\underline{x}_0$. However, this is a special case. Therefore, without sufficient high speed computing power, time optimal sampled-data control is impractical for our case.

3.3.2 Sampled-data — quadratic performance index problem

Given the sampled-data state equation, the quadratic performance index control problem requires that the optimal control law m(k), for k = 0, 1, 2, ..., N - 1, be found such that the quadratic performance index

$$I_N = \sum_{k=1}^{N} [\underline{x}^T(k)Q\underline{x}(k) + \lambda r(k-1)m^2(k-1)] = \sum_{k=1}^{N} [QI] \tag{3-36}$$

is minimized and where Q is a positive definite matrix, $r > 0$ and $\lambda > 0$, with the system transferred from a state $\underline{x}_0$ to a final state $\underline{x}(N) = 0$. For notational convenience, T has been defined equal to one without loss of generality. This transference is called an N-stage process.

Define

$$f_N[\underline{x}(0)] = \min_{\substack{m(0) \\ \vdots \\ m(N-1)}} I_N \tag{3-37}$$

and the return for the last N - j stages of the N-stage process to be

$$f_{N-j}[\underline{x}(j)] = \min_{\substack{m(j) \\ \vdots \\ m(N-1)}} I_{N-j} = \min_{\substack{m(j) \\ \vdots \\ m(N-1)}} \sum_{k=j+1}^{N} [QI] \quad \text{for} \quad j = 0, 1, 2, \ldots, N-1. \tag{3-38}$$

Applying the principle of optimality, which states that each segment of an optimal trajectory is optimal, i.e., an optimal function of its last state,

$$f_{N-j}[\underline{x}(j)] = \min_{m(j)} \{\underline{x}^T(j+1)Q\underline{x}(j+1) + rm^2(j) + f_{N-(j+1)}[\underline{x}(j+1)]\} \quad . \tag{3-39}$$

Using the induction hypothesis, it can be shown that the minimum performance index for the last N - j stages can be expressed as

$$f_{N-j}[\underline{x}(j)] = \underline{x}^T(j)P(N-j)\underline{x}(j) \quad . \tag{3-40}$$

This form can be used to determine a tentative solution where P(N-j) is a symmetric matrix. Similarly, the minimum value of the performance index for the last N - j + 1 stages is

$$f_{N-(j+1)}[\underline{x}(j+1)] = \underline{x}^T(j+1)P(N-j-1)\underline{x}(j+1) \quad . \tag{3-41a}$$

Substituting Eq. (3-41a) into Eq. (3-39), we obtain

$$f_{N-j}[\underline{x}(j)] = \min_{m(j)} [\underline{x}^T(j+1)V(N-j-1)\underline{x}(j+1) + \lambda rm^2(j)] \tag{3-41b}$$

where

$$V(N-j-1) = Q + P(N-j-1) \quad . \tag{3-42}$$

Substituting the state transition equation for $\underline{x}(j+1)$ into (3-41b) and carrying out the implicit multiplication,

$$f_{N-j}[\underline{x}(j)] = \min[\underline{x}^T(j)V_{\phi\phi}(N-j-1)\underline{x}(j) + m(j)V_{\theta\phi}(N-j-1)\underline{x}(j) + \underline{x}^T(j)V_{\phi 0}(N-j-1)m(j) + V_{00}(N-j-1)m^2(j)] \tag{3-43}$$

where

$$V_{\phi\phi}(\cdot) = \Phi(1)V(\cdot)\Phi(1)$$

$$V_{\theta\phi}(\cdot) = \Theta(1)V(\cdot)\Phi(1)$$

$$V_{\phi\theta}(\cdot) = \Phi(1)V(\cdot)\Theta(1)$$

$$V_{\theta\theta}(\cdot) = \Theta(1)V(\cdot)\Theta(1) \quad .$$

So to find the minimum, let us take the partial derivative of $f_{N-j}[\underline{x}(j)]$ with respect to m(j) and equate it to zero. After some calculation, we find that the optimal m(j) is

$$m^{O}(j) = [V_{\theta\theta}(N-j+1) + \lambda r]^{-1} V_{\theta\phi}(N-j+1)\underline{x}(j) \tag{3-44}$$

or defining H(N-j), Eq. (3-44) simplifies to

$$m^{O}(j) = H(N-j)\underline{x}(j) \quad . \tag{3-45}$$

Note that the term in the $[]^{-1}$ of Eq. (3-44) is a scalar. Substituting $m^{O}(j)$ into Eq. (3-43), we find that

$$f_{N-j}[\underline{x}(j)] = \underline{x}^{T}(j)[V_{\phi\phi}(N-j-1) + V_{\phi\theta}(N-j-1)]\underline{x}(j) \quad , \tag{3-46}$$

by using the symmetry properties of $V_{\phi\theta} + V_{\theta\phi}$ and their resultant effect on H and H^{T}.

Hence, from Eq. (3-40),

$$P(N-j) = V_{\phi\phi}(N-j-1) + V_{\phi\theta}(N-j-1)H(N-j) \quad . \tag{3-47}$$

Substituting for the V_{xx}'s in terms of Φ's and Θ's

$$P(N-j) = \Phi^T(1)[Q + P(N-j-1)][\Phi(1) + \Theta(1)H(N-j)] \tag{3-48}$$

where

$$H(N-j) = -\{\Theta^T(1)[Q + P(N-j-1)]\Theta(1) + \lambda r\}^{-1}\Theta^T(1)[Q + P(N-j-1)]\Phi(1) \quad . \tag{3-49}$$

Therefore, $P(k)$ is defined for $k = 0, 1, \ldots, N - 1$, where $P(0) = 0$. These two equations for $P(\cdot)$ and $H(\cdot)$ form the recursive relationship needed to calculate the $\underline{x}(j)$'s and $m(j)$'s from the following two equations:

$$m(j) = H(N-j)\underline{x}(j) \tag{3-50}$$

and the state equation

$$\underline{x}(j+1) = \Phi(1)\underline{x}(j) + \Theta(1)m(j)$$

We note that for the initial $\underline{x}(0)$, $P(0)$ is given so that $H(1)$ can be calculated from Eq. (3-49). $P(1)$ can be then calculated from Eq. (3-48) using $H(1)$. This process continues until $H(N)$ is calculated. Then it is substituted in reverse-subscript order into Eq. (3-45) to give the control $m(k)$ at each stage $k = 0, \ldots, N - 1$ to form the control sequence to drive the system to $\underline{x}(N) = \underline{0}$ in N sampling periods.

Again, there is a great deal of computation involved, first to calculate $H(j)$ in reverse time and then to calculate $m(j)$ in forward time. We are fortunate that the inverse in the $\{\}$ brackets in the equation for $H(N-j)$, Eq. (3-49), is a scalar, thereby eliminating the

need for a matrix inversion. Nevertheless, unless a great deal of computation power is available, the time delay to start the control process may be intolerable.

3.4 Time Optimal Variable Sampling Interval Problem Using the Maximum Principle

Let us consider the time optimal sampled-data problem with a variable sampling period from the perspective of the Maximum Principle [141]. To do this, by use of the similarity transform, let us convert the dynamics described by Eq. (3-12) to a diagonalized set of dynamics

$$\dot{\underline{z}} = \Lambda \underline{z} + \Gamma m \tag{3-51}$$

where

$$\Lambda = \begin{vmatrix} 0 & 0 & 0 \\ 0 & \lambda_1 & 0 \\ 0 & 0 & \lambda_2 \end{vmatrix} \quad \lambda_2 < \lambda_1 < 0 \text{ are nonzero roots of the characteristic equation.} \tag{3-52}$$

$$\Gamma = \left[\frac{\eta}{\alpha_0} , \frac{y_{1e} e^{\eta\lambda_2}}{y_{3e}\alpha_1(\lambda_1 - \lambda_2)} , \frac{y_{1e} e^{\eta\lambda_1}}{y_{3e}\alpha_2(\lambda_1 - \lambda_2)} \right]^T \tag{3-53}$$

$$\alpha_0 = \sqrt{\frac{1}{1 + 2\left(\frac{y_{1e}}{y_{3e}}\right)^2}} \tag{3-54a}$$

$$\alpha_i = \sqrt{\frac{1}{1 + \left(\frac{\lambda_i + a_{21}}{a_{21}}\right)^2}} \quad \text{for} \quad i = 1, 2 \quad . \tag{3-54b}$$

With the definition of the time optimal performance index, the Hamiltonian function is:

$$H = 1 + p_2\lambda_1 z_2 + p_3\lambda_2 z_3 + m(t)[\Gamma_1 p_1 + \Gamma_2 + p_2 + \Gamma_3 p_3] \tag{3-55}$$

where p_i, i = 1, 2, 3, are the adjoint variables whose dynamic equations are

$$\frac{\partial H}{\partial \underline{z}} = \dot{\underline{p}} = [0, \lambda_1 p_2, \lambda_2 p_3]^T \quad . \tag{3-56}$$

The solutions of these equations are:

$$p_1(t) = C_1 \tag{3-57a}$$

$$p_2(t) = C_2 \exp(\lambda_1 t) \tag{3-57b}$$

$$p_3(t) = C_3 \exp(\lambda_2 t) \tag{3-57c}$$

where C_i are constants of integration, $C_i = p_i(0)$. Therefore, for some combination of C_i's, it is possible that the function $M(t) = \Gamma_1 p_1 + \Gamma_2 p_2 + \Gamma_3 p_3$ can have at most two zeros. Now the control that minimizes H is:

$$m(t) = \text{sgn}[\Gamma_1 p_1 + \Gamma_2 p_2 + \Gamma_3 p_3] = \text{sgn}[M(t)] \quad . \tag{3-58}$$

Hence, m(t) can have at most two switchings.

Since the magnitude of m is constant and only the sign changes over time, let us define

$$m(t) = \sigma = \pm 1 \tag{3-59}$$

and solve the diagonalized dynamics

$$z_1(t) = z_1(0) + \beta_1(\sigma)t \tag{3-60a}$$

$$z_2(t) = \beta_2(\sigma)t + z_2(0)e^{\lambda_2 t} \tag{3-60b}$$

$$z_3(t) = \beta_3(\sigma)t + z_3(0)e^{\lambda_2 t} \tag{3-60c}$$

where

$$\beta_1(\sigma) = \frac{\eta\sigma}{\alpha_0} \tag{3-61a}$$

$$\beta_2(\sigma) = \frac{y_{1e}\eta\lambda_1\sigma}{y_{3e}\alpha_1(\lambda_1 - \lambda_2)} \tag{3-61b}$$

$$\beta_3(\sigma) = \frac{y_{1e}\eta\lambda_2\sigma}{y_{3e}\alpha_1(\lambda_1 - \lambda_2)} \quad . \tag{3-61c}$$

From these equations, the phase-plane relationships can be derived. For the z_1 - z_2 phase plane, projection of the trajectory is

$$z_2(t) = \gamma_2[z_1 - z_1(0)] + z_2(0)\exp\{\delta_2(\sigma)[z_1 - z_1(0)]\} \tag{3-62}$$

where

$$\gamma_2 = \frac{y_{1e}\alpha_0\lambda_1}{y_{3e}\alpha_1(\lambda_1 - \lambda_2)} \approx \frac{\lambda_1}{\lambda_2}\frac{1}{\sqrt{2}\,\alpha_1} \tag{3-63}$$

$$\delta_2(\sigma) = \frac{\lambda_1\alpha_0}{\eta\sigma} \approx \frac{\lambda_1}{\sqrt{2}}\frac{y_{3e}}{y_{1e}}\sigma \quad . \tag{3-64}$$

Similarly, in the z_1 - z_3 phase plane,

$$z_3(t) = \gamma_3[z_1 - z_1(0)] + z_3(0)\exp\{\delta_3(\sigma)[z_1 - z_1(0)]\} \tag{3-65}$$

where

$$\gamma_3 = \frac{y_{1e}\alpha_0\lambda_2}{y_{3e}\alpha_1(\lambda_1 - \lambda_2)} \approx -\frac{1}{\sqrt{2}\,\alpha_2} = -\sqrt{\frac{1 + \frac{(\lambda_2 + a_{21})}{a_{21}}}{2}} \tag{3-66a}$$

$$\delta_3(\sigma) = \frac{\lambda_2\alpha_0}{\eta\sigma} \approx \frac{\lambda_2}{\sqrt{2}}\frac{y_{3e}}{y_{1e}}\,\sigma \tag{3-66b}$$

The equation for the z_2 - z_3 phase plane involves the solving of two simultaneous transcendental equations. Its solution would serve no useful purpose here and, hence, will not be included.

Now let us define

t_1 = first switching time

t_2 = second switching time

t_f = final switching time

and

$$T_1 = t_1 - t_0 \tag{3-67a}$$

$$T_2 = t_2 - t_1 \tag{3-67b}$$

$$T_3 = t_f - t_2 \tag{3-67c}$$

assuming that the first control is applied at $t = t_0 = 0$.
Assuming two switchings for generality, the control sequence is given by

$$m(t) = \{\sigma, -\sigma, \sigma\} \quad . \tag{3-68}$$

Thus, at the first switching point at $t = t_1$, the values of $\underline{z}$ become

$$z_1(t_1) = z_1(t_0) + \beta_1(\sigma)T_1 \tag{3-69a}$$

$$z_2(t_1) = z_2(t_0)\exp(\lambda_1 T_1) + \beta_2(\sigma)T_1 \tag{3-69b}$$

$$z_3(t_1) = z_3(t_0)\exp(\lambda_2 T_1) + \beta_3(\sigma)T_1 \quad . \tag{3-69c}$$

Similarly, at the second switching point at $t = t_2$,

$$z_1(t_2) = z_1(t_1) - \beta_1(-\sigma)T_2 \tag{3-70a}$$

$$z_2(t_2) = z_2(t_1)\exp(\lambda_1 T_2) - \beta_2(-\sigma)T_2 \tag{3-70b}$$

$$z_3(t_2) = z_3(t_1)\exp(\lambda_2 T_2) - \beta_3(-\sigma)T_2 \tag{3-70c}$$

and at the final point $t = t_f$,

$$z_1(t_3) = z_1(t_2) + \beta_1(\sigma)T_3 = 0 \tag{3-71a}$$

$$z_2(t_3) = z_2(t_2)\exp(\lambda_1 T_3) + \beta_2(\sigma)T_3 = 0 \tag{3-71b}$$

$$z_3(t_3) = z_3(t_2)\exp(\lambda_2 T_3) + \beta_3(\sigma)T_3 = 0 \quad . \tag{3-71c}$$

Solving the above sets of equations for T_3,

$$T_3 = T_2 - T_1 + \frac{\alpha_0}{n\sigma} z_1(t_0) \geq 0 \tag{3-72a}$$

other equations in terms of $\underline{z}(t_0)$, and T_i's can be found,

$$z_3(t_0) = -\beta_3(\sigma)\left[T_2 - T_1 + \frac{z_1(t_0)}{\beta_1(\sigma)}\right]e^{-\lambda_2\left(2T_2 + \frac{z_1(t_0)}{\beta_1(\sigma)}\right)}$$

$$+ \beta_3(\sigma)T_2 e^{-\lambda_2(T_2+T_1)} - \beta_3(\sigma)T_1 e^{-\lambda_2 T_1} \qquad (3\text{-}72b)$$

$$z_2(t_0) = -\beta_2(\sigma)\left[T_2 - T_1 + \frac{z_1(t_0)}{\beta_1(\sigma)}\right]e^{-\lambda_1\left(2T_2 + \frac{z_1(t_0)}{\beta_1(\sigma)}\right)}$$

$$+ \beta_2(\sigma)T_2 e^{-\lambda_1(T_2+T_1)} - \beta_2(\sigma)T_1 e^{-\lambda_1 T_1} \qquad (3\text{-}72c)$$

The above two equations are a set of simultaneous transcendental equations of given constants and the variables T_1, T_2, under the obvious constraints $T_1 \geq 0$, $T_2 \geq 0$.

For the solution of Eq. (3-72), the T_i's apply whether or not one is using the x or z coordinates. However, to get the initial conditions of $\underline{z}$ used in the solution, it is necessary to use the similarity transform on the initial conditions of $\underline{x}$. This is not computationally difficult, particularly if the similarity transform has already been calculated beforehand. The solution still involves the solution of simultaneous transcendental equations, a nontrivial computation problem from the microprocessor's perspective. Nevertheless, it may soon be less of a problem as the state of the art of microprocessors advances.

3.5 Summary

The analysis of this chapter was predicated upon possible microprocessor implementation of the controller. First considered was a continuous time optimal controller. The form of the control was complex but implementable. Also implementable was the continuous quadratic performance index controller.

Sampled-data controllers were next considered. The time optimal formulation was found to have implementation difficulties, due to the great amount of computation necessary to define which complex polygon contains the initial state. The quadratic performance index formulation involves a great deal of computation for small sampling intervals.

Finally, the application of the Maximum Principle to the time optimal problem yields a computationally difficult solution. However, after the computations are made, the controller is relatively simple to implement.

Several observations should be offered. First, control problems require a substantial amount of computation before the control process actually begins to operate. When implemented, these initial calculations may take from several seconds to a few minutes depending upon which type of control is used. After these initial calculations are completed and the control initiated, there are computations necessary to continue the control process. The only exception to this is the Maximum Principle solution where the switching times are initially calculated with the sign of the control so that only a timer is needed to implement it. The computations required and their difficulty are summarized in Table 5. The terms used in this table are qualitative in nature to give a relative

TABLE 5

COMPARISON OF THE CONTROL STRATEGIES ANALYZED IN CHAPTER 3

	Computational Difficulty Scale (1-10)	Computations Required		Knowledge of Initial State Only Needed	Possible to Exceed the Rate of Change in Ventilation Constraint
		Initial	Continuous		
Continuous Time Optimal	5	Large	Moderate	No	No
Continuous Quadratic Index	7	Large	Small	No	Yes
Sampled Data Time Optimal	9	Very Large	Small*	Yes*	No
Sampled Data Quadratic Index	6	Large	Small*	Yes*	Yes
Maximum Principle Time Optimal	4	Large	None	Yes	No

* Knowledge of states at the sampling interval could be used in calculation of the control for that interval; however, it is not really necessary.

comparison. The specific state of the art of microprocessors and numerical techniques at later time could change these relative values.

It is important to note that the values of the Q matrix and r in the performance index are important. If they are chosen inappropriately, the constraint of the time rate of change of the ventilation could be violated.

4. FUTURE WORK

The state of the art of respiratory monitoring and transducer technology supporting respiratory monitoring in the mid-seventies is equivalent to that of cardiovascular technology and monitoring in the mid-sixties. The transducer technology is enabling transducers to be developed that are small, easy to handle, and give consistent measurements. This, in turn, is allowing physiologists and clinicians to develop new monitoring techniques. These newly developed techniques, in turn, improve patient care by increasing the availability of respiratory monitoring and facilitating early detection of developing pathology.

Until quite recently, a respirator control system was not feasible, due to the expense of the electronic components required and the inadequate transducer technology. Taking the work of Chapter 3, and developing a suboptimal controller is the next step. As can be seen from the complexity of some of the solutions of control problems, a simpler suboptimal solution is more easily implemented. Since acceptable measurement errors of physiological functions are on the order of one to three percent, an approximate suboptimal solution should easily fall within these limits of error. In addition, the amount of electronics, or the computing power, or both, that is required, will be less than that of the typical engineering application.

The form of implementation of the suboptimal control could take several directions. A desk calculator system similar to the one that Turney et al. [115] uses may be one direction. A hybrid analog/digital computer could be used. Similarly, a minicomputer with appropriate peripherals

is also feasible. With the new Large-Scale Integration (LSI) integrated circuit devices being developed, a microprocessor with several LSI chips performing the signal preprocessing is a most feasible implementation.

Whatever form the implementation takes, the controller will be controlling the carbon dioxide gas exchange, assuming that the patient is adequately oxygenated. This may not be the case. Therefore, a sensing device validating the assumption is required. Fortunately, an oxymeter that fits noninvasively over the earlobe has been developed recently. Its accuracy is not high, but enough to ensure that the oxygenation assumption is not violated. After additional development, an integrated controller for both oxygen and carbon dioxide regulation may become feasible. In addition, a direct result of the carbon dioxide regulator is the measure of pulmonary mechanics. This can be used to refine the regulatory process, as well as provide immediate information for the physician to assess the patient's condition.

The present form of the regulator, when implemented, is illustrated in Fig. 13. It uses respiratory parameter measuring circuitry to monitor the pulmonary mechanics and the gas exchange parameters. The state estimator is used to detect alarm conditions and estimate the arterial Pco_2. It will be allowed to vary such parameters as inspiration/expiration ratio, peak pressure, and peak flow to insure that the desired ventilation is delivered. The state regulator will determine basic alveolar ventilation from the estimated arterial carbon dioxide and the desired level, by varying the basic control parameters — tidal volume and frequency — and using a deadspace estimation from the airway measurements.

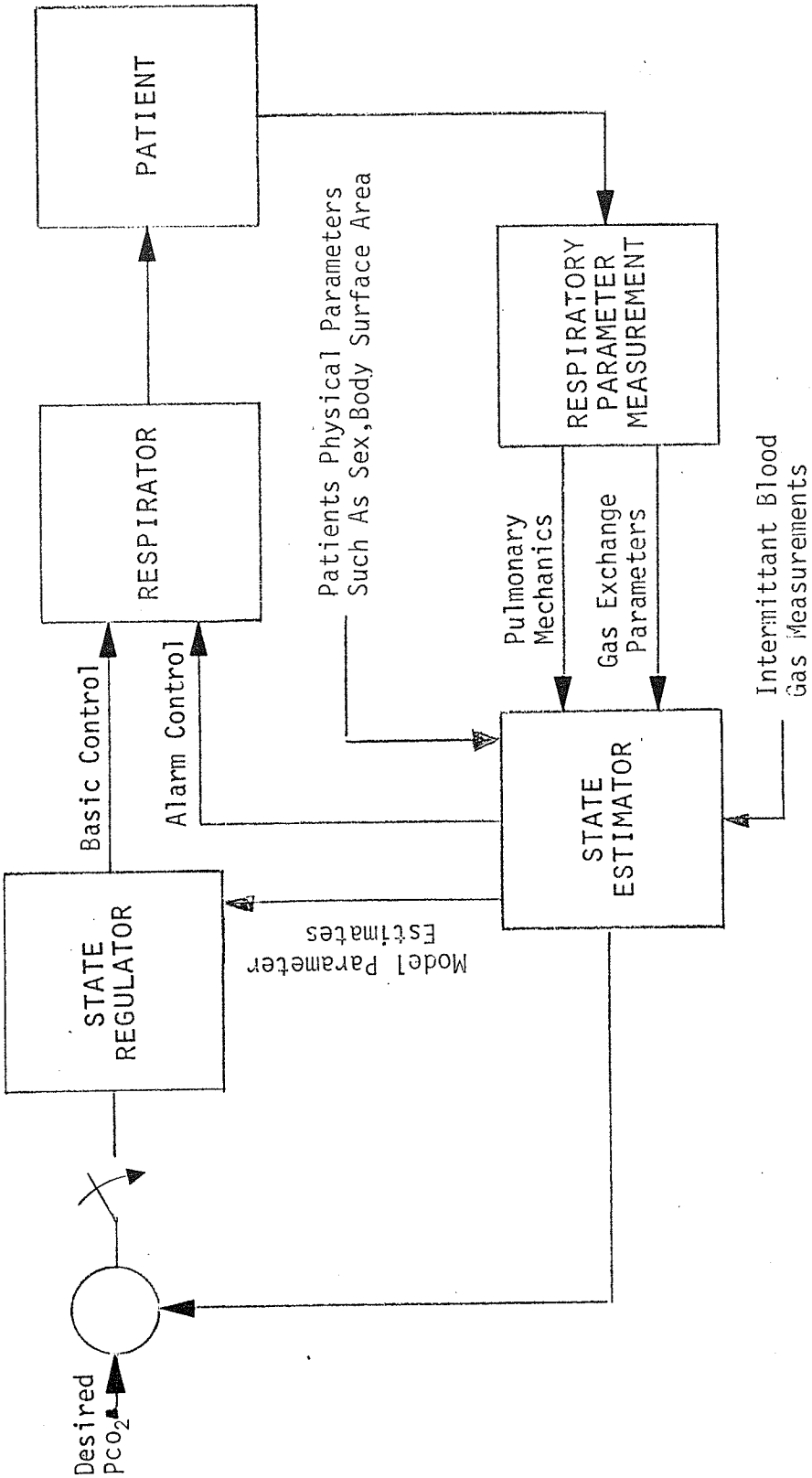

Figure 13. Basic respirator control system.

The parameters of the physiological model are a fundamental cause for future concern. They will be estimated. However, due to the general uncertainties of dealing with an abnormal physiology, with a general model, these parameter estimates may be in error. Nevertheless, the sensitivity of the model to these possible errors should be minimized by the fact that an erroneous estimate will cause either or both of the optimal and suboptimal controller solutions to force the carbon dioxide levels within the neighborhood of the desired level. After reaching the neighborhood of the desired $\underline{x}_f$, the tidal volume and frequency will be incrementally adjusted to achieve the desired carbon dioxide levels.

Figure 14a illustrates the optimal solution's trajectory in a coordinate system of the alveolar carbon dioxide level, the tidal volume and frequency of respiration. Note the bounds of tidal volume and frequency are physician set for clinical reasons. It is important to note that if the trajectory of the optimal solution, using the estimated parametric values, does not achieve a position within the neighborhood of the desired $P_A co_2$, the control will have extreme values of tidal volume and frequency corresponding to the corners of the cube in the figure. If that case ever occurs, the parametric estimates must be sufficiently in error so that physician intervention is required. The control system will signal attending personnel of such a need.

Figure 14b illustrates the approach of the optimal trajectory to the neighborhood of the desired value and the takeover by a neighborhood control to achieve the desired value of carbon dioxide. This neighborhood control law is of a parameter-insensitive form following the work of Utkin [142].

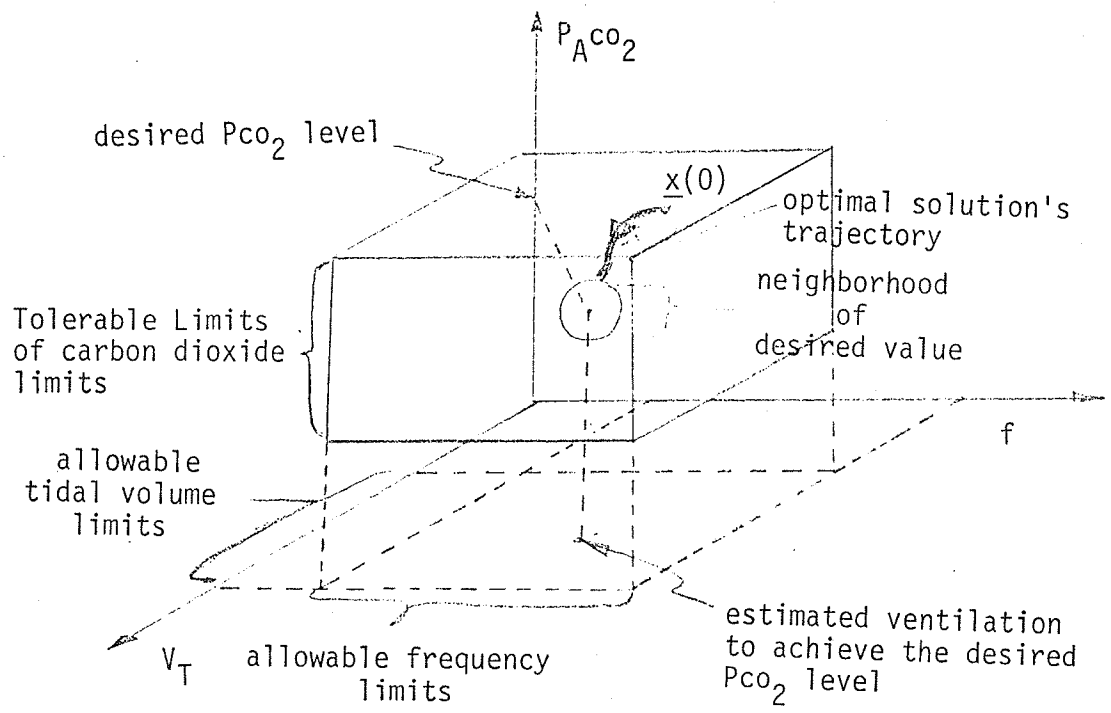

Figure 14a. Bounds of the system states.

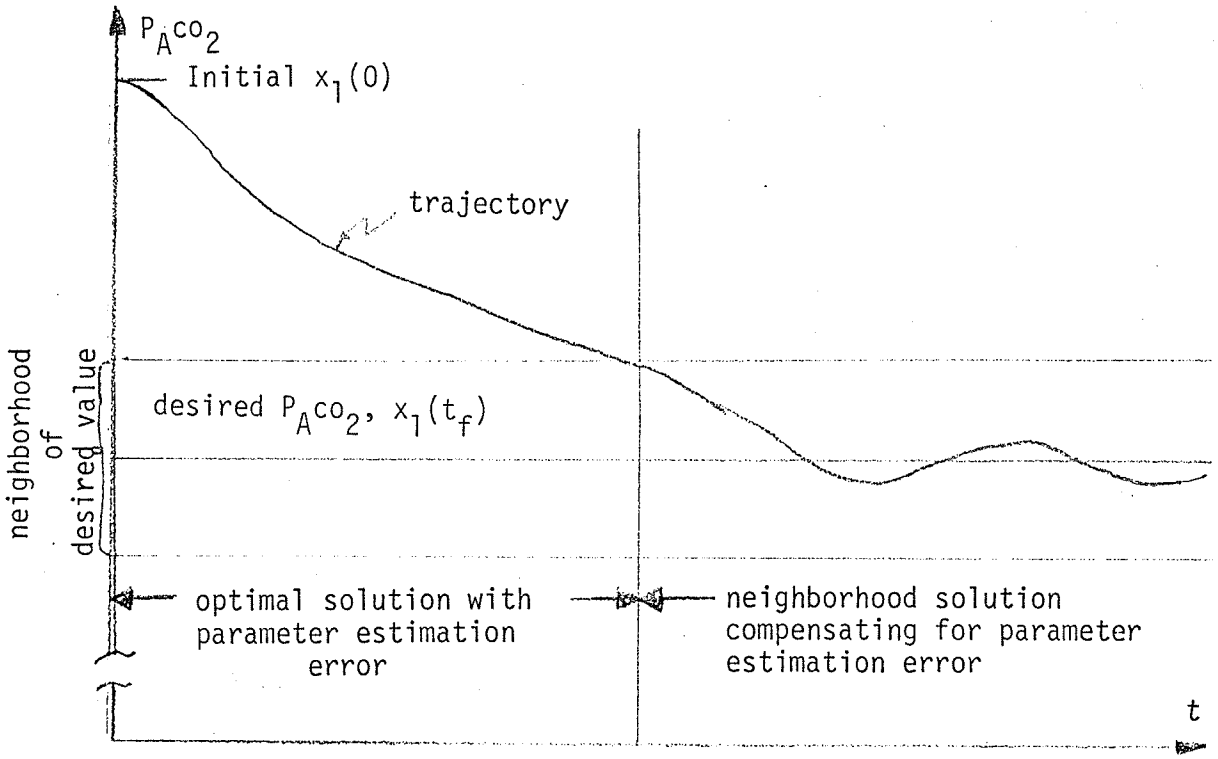

Figure 14b. System compensation for parameter estimation error.

Any other future refinements of the controller would involve the use of pulmonary mechanics to improve model parameter estimates. As the medical community gets more experience with the improved transducers, new and more refined estimates of pulmonary function should make a great impact upon the controller.

5. SUMMARY AND CONCLUSIONS

As we have seen from Chapter 1, the human respiratory system is very complex. Many of the sites of elements of it and their effect still have to be identified to improve the fidelity of respiratory system models. Since the goal of this dissertation was to develop a viable model of respiratory function, as a basis for respirator control, the refinement of models of normal physiology was considered tangential to the problem. Instead, the use of conservation principles was applied to the physiology to obtain a simple model, which can be used in the design of a respirator control system. Various formulations of optimal control problems were utilized to find the solution that could be most readily implemented on a microprocessor. Several were found.

Much research into respirator control systems is left to be done. The technology is available to implement them. More data must be obtained from the clinical environment to help refine the implementation of such a control system. However, the time is right for such a development.

LIST OF REFERENCES

1. Radford, E. P., "Ventilation Standards for Use in Artificial Respiration," J. Appl. Physiol., 7, 451-460, 1955.

2. Peters, R. M., The Mechanical Basis of Respiration, Little, Brown and Company, Boston, 1969.

3. Nunn, J. F., Applied Respiratory Physiology, Appleton-Century-Crofts, New York, 1969.

4. Grogono, A. W. and Byles, P. H., "Mechanical Ventilators," in Dobkin, A. B. (ed.), Ventilators and Inhalation Therapy, 2nd ed., Little, Brown and Company, Boston, 1972.

5. Mead, J., "Mechanical Properties of the Lungs," Physiol. Rev., 41, 281-330, 1961.

6. Jain, V. K. and Guha, S. K., "A Control System for the Long-Term Ventilation of the Lungs," IEEE Trans., BME-19, 47-53, 1972.

7. Pontoppidan, H., "Prolonged Artificial Ventilation, a Quantitative Approach," Postgrad. Med., 37, 576-583, 1965.

8. Hilberman, M., Stacy, R. W. and Peters, R. M., "A Phase Method of Calculating Respiratory Mechanics Using a Digital Computer," J. Appl. Physiol., 32, 535-541, 1972.

9. Wald, A. A., Murphy, T. W. and Mazzia, V. D. B., "A Theoretical Study of Controlled Ventilation," IEEE Trans., BME-15, 237-248, 1968.

10. Moore, F. D., Lyons, Jr., J. H., Peirce, Jr., E. C., Morgan, Jr., A. P., Drinker, P. A., MacArthur, J. D. and Dammin, G. J., Post-Traumatic Pulmonary Insufficiency, W. B. Saunders, Philadelphia, 1969.

11. Bendixen, H. H., "Rational ventilator modes for respiratory failure," Crit. Card Med., 2, 225-227, 1974.

12. Anderson, M. N., "Ventilatory Support," Surgery, 66, 1112-1129, 1969.

13. Peters, R. M. and Hutchin, P., "Adequacy of Available Respirators to Their Tasks," Annl. Thorac. Surg., 3, 414-430, 1967.

14. Whittenberg, J. L. (ed.), Artificial Respiration, Hoeber Medical Division, Harper and Row, New York, 1962.

15. Norlander, O. P., "The Use of Respirators in Anesthesia and Surgery," Acta. Anaesth. Scand., Suppl., 30, 5-74, 1968.

16. Hilberman, M., Patitucci, P. J. and Peters, R. M., "On-line Assessment of Cardiac and Pulmonary Pathophysiology in the Acutely Ill," J. Assoc. Adv. Med. Instr., 6, 65-69, 1972.

17. Osborne, J. J., Beaumont, J. O., Raison, J. C. A., Russell, J. and Gerbode, F., "Measurements and Monitoring of Acutely Ill Patients by Digital Computer," Surgery, 64, 1057-1070, 1968.

18. Turney, S. Z., Blumenfeld, W., Wolf, S. and Denman, R., "Respiratory Monitoring," Annals of Thoracic Surgery, 16, 184-191, 1973.

19. Mikami, T. and Yoshimoto, C., "Minimum Energy Control of Human Respiration," Japanese Journal of Medical Electronics and Biological Engineering, 4, 12-21, 1966.

20. Peters, R. M., "Energy Cost (Work) of Breathing," Annl. Thorac. Surg., 7, 51-67, 1969.

21. Yamashiro, S. M., "Regulation of the Mammalian Respiratory System," Ph.D. Dissertation, Biomedical Engineering Department, University of Southern California, Los Angeles, California, 1970.

22. Comroe, J. H., Physiology of Respiration, Yearbook Medical Publishers, Chicago, 1965.

23. DeJours, P., Respiration, Oxford University Press, New York, 1966, L. E. Farhi (Translator).

24. Gray, J. S., "The Multiple Factor Theory of the Control of Respiratory Ventilation," Science, 103, 739-744, 1946.

25. Grodins, F. S., Gray, J. S., Schroder, K. R., Norins, A. L. and Jones, R. W., "Respiratory Responses to CO_2. A Theoretical Study of a Non-Linear Biological Regulator," J. Appl. Physiol., 7, 283-308, 1954.

26. Mikic, B. B., Benn, J. A. and Drinker, P. A., "Upper and lower bounds on Oxygen transfer Rates: A theoretical Consideration," Annals of Biomedical Engineering, 1, 212-220, 1972.

27. Yamamoto, W. S. and Raub, W. F., "Models of the Regulation of External Respiration in Mammals. Problems and Promises," Computers and Biomedical Research, 1, 65-104, 1967.

28. Riggs, D. M., Control Theory and Biological Feedback Mechanisms, Dover, N.Y., (pp 401-418), 1970.

29. Horgan, J. D. and Lange, R. L., "Chemical Control in the Respiratory System," IEEE Trans., BME-15, 119-127, 1968.

30. Defares, J. G., Derksen, H. E. and Duyff, J. W., "Cerebral Blood Flow in the Regulation of Respiration," Acta. Physiol. Pharmacol. Neerlandica, 9, 327-360, 1960.

31. Defares, J. G., "Principles of Feedback Control and Their Application to the Respiratory Control System," Handbook of Physiology, Respiration, Vol. 1, Fenn, W. O. and Rahn, H. (eds.), American Physiological Society, Washington, D.C., 1964.

32. Grodins, F. S. and James, G., "Mathematical Modesl of Respiratory Regulation," N. Y. Acad. Sci. Ann., 109, 852-868, 1963.

33. Grodins, F. S., Buel, J. and Bart, A. J., "Mathematical Analysis and Digital Simulation of the Respiratory Control System," J. Appl. Physiol., 22, 260-276, 1967.

34. Priban, I. P. and Fincham, W. F., "Self-Adaptive Control and the Respiratory System," Nature, 208, 339-343, 1965.

35. Priban, I. P., "Self-Adaptive Respiratory Control," Breathlessness, Howell, J. B. L. and Campbell, E. M. J. (eds.), Philadelphia, Davis, 1966.

36. Hey, E. H., Lloyd, B. B., Cunningham, D. C. J., Hukes, M. G. G. and Bolton, D. P. G., "Effects of Various Respiratory Stimuli on the Depth and Frequency of Breathing Man," Respiratory Physiology, 1, 193-205, 1966.

37. Mathews, C. M. E., Laszlo, G., Campbell, E. J. M. and Read, D. J. C., "A Model for the Distribution and Transport of CO_2 in the Body and the Ventilation Response to CO_2," Respiratory Physiology, 6, 45-87, 1969.

38. Horgan, J. D. and Lange, R. L., "Analog Computer Studies of Periodic Breathing," I.R.E. Trans. Bio-Medical Electronics, 9, 221-228.

39. Horgan, J. D. and Lange. R. L., "Digital Computer Simulation of the Human Respiratory System," IEEE International Convention Record, Part 9, 149-157, 1963.

40. Horgan, J. D. and Lange, R. L., "A Model of the Respiratory Control System Which Includes the Effect of Cerebro-spinal Fluid and Brain Tissue," Proc. Ann. Conf. Engrg. in Med. and Biol., 6, 10, 1964.

41. Milhorn, Jr., H. T., Benton, R., Ross, R. and Guyton, A. C., "A Mathematical Model of the Human Respiratory Control System," Biophys. J., 5, 27-46, 1965.

42. Milhorn, Jr., H. T. and Brown, D. R., "Steady-State Simulation of the Human Respiratory System," Computers and BioMedical Res., 4, 604-619, 1971.

43. Milhorn, Jr., H. T., Reynolds, W. J. and Holloman, Jr., G. H., "Digital Simulation of the Ventilatory Response of CO_2 Inhalation and CSF Perfusion," Computers and BioMedical Research, 5, 301-314, 1973.

44. Reynolds, W. J., Milhorn, Jr., H. T. and Holloman, Jr., G. H., "Transient Ventilatory Response to Graded Hypercapnia in Man," J. Appl. Physiol., 33, 47-54, 1972.

45. Mead, J., "Control of Respiratory Frequency," J. Appl. Physiol., 15, 325-336, 1960.

46. Ruttimann, U. E. and Yamamoto, W. S., "Respiratory airflow patterns that satisfy power and force criteria of optimality," Computers and BioMedical Research, 5, 146-159, 1972.

47. West, J. B., Ventilation/Blood Flow and Gas Exchange, Blackwell Scientific Publications, Oxford, 1965.

48. West, J. B., "Ventilation-Perfusion Inequality and Overall Gas Exchange in Computer Models of the Lungs," Respir. Physiol., 7, 88-110, 1969.

49. Peters, R. M., "Coordination of Ventilation and Perfusion," Ann. Thorac. Surg., 6, 570-590, 1968.

50. Bergman, N. A., "Effect of Respiratory Waveforms on Distribution of Inspired Gas During Artificial Ventilation," Amer. Rev. Resp. Dis., 100, 518-525, 1969.

51. West, J. B., "Topographical Distribution of Blood Flow in the Lung," Fen, W. O., and Rahn, H. (eds.), Hnbk. of Physiol., Amer. Physiol. Soc., Washington, D.C., 1964.

52. Crane, H. D., "Bubbles, Balloons, Capillaries, and Alveoli," S.R.I. Journal, 28-48, 1969.

53. Clements, J. A., "Surface Tension in the Lungs," Scientific American, 207, 121-148, December 1962.

54. Clements, J. A., "Surface Phenomena in Relation to Pulmonary Function," Physiologist, 5, 11-28, 1962.

55. Tierney, D. F., "Lung Metabolism and Biochemistry," Ann. Rev. of Physiol., 36, 209-232, 1974.

56. Bendixen, H. H., Hedley-White, J. and Laver, M. B., "Impaired Oxygenation in Surgical Patients During General Anesthesia with Controlled Ventilation. A Concept of Atelectasis," New Eng. J. Med., 269, 991-996, 1963.

57. Bendixen, H. H., "Atelectasis and Shunting," Anesthesiology, 25, 595-596, 1964.

58. Laver, M. B. and Bendixen, H. H., "Atelectasis in the Surgical Patient, Recent Conceptual Advances," Progr. Surg., 5, 1-32, 1965.

59. Sterling, G. M., "The Mechanism of Broncoconstriction Due to Hypocapnia in Man," Clin. Sci., 34, 277-285, 1968.

60. Patterson, R. W., Sullivan, S. F., Malm, A. R. and Bowman, Jr., F. O., "Comparison of Effects of Airway Versus Systemic Carbon Dioxide Tension on Human Airway Mechanics," J. Thoracic and Cardiovas. Surg., 58, 209-216, 1969.

61. Yamashiro, S. M. and Grodins, F. S., "Optimal Regulation of Respiratory Airflow," J. Appl. Physiol., 30, 597-602, 1971.

62. Widdicombe, J. G. and Nadel, J. A., "Airway Volume, Airway Resistance, and Work and Force of Breathing: Theory," J. Appl. Physiol., 18, 863-868, 1963.

63. Korta, L. B., Horgan, J. D. and Lange, R. L., "Stability Analysis of the Human Respiratory System," Proc. of N.E.C., 15, 201-206, 1965.

64. Defares, J. G., Hara, H. H. and Billinghurst, E. M., "The Stability of the Respiratory Servomechanism: An Analog Computer Study," Prog. in Biocybernetics, 1, 109-123, 1964.

65. Ashby, W. R., Personal Communication.

66. Stoll, P. J. and Meditch, J. S., "Least Squares Estimation of Respiratory System Parameters," Mathematical Biosciences, 8, 307-321, 1970.

67. Chick, D. R., "Digital Techniques for the Approximate Identification and Simulation of the Respiratory-Heartrate System," Ph.D. Dissertation, University of Texas, Austin, Texas, 1970.

68. Stoll, P. J., "Respiratory System Analysis Based on Sinusoidal Variations of CO_2 in Inspired Air," J. Appl. Physiol., 27, 389-399, 1969.

69. Yamamoto, W. S., "Theory of Measurement of Respiratory Response," J. Appl. Physiol., 25, 439-446, 1968.

70. Yamamoto, W. and Nori, T., "Phasic Air Movement Model of Respiratory Regulation of Carbon Dioxide Balance," Computers and Biomedical Res., 3, 699-717, 1970.

71. Yamashiro, S. M., Grodins, F. S. and Sohrab, S., "Simulation of Respiratory Responses to Sinusoidally Varying Inspired FCO_2," Proc. of San Diego Biomedical Symposium, 12, 33-36, 1972.

72. Goldman, M., Knudson, R. J., Mead, J., Peterson, N., Schwaber, J. R. and Whol, M. E., "A Simplified Measurement of Respiratory Resistance by Forced Oscillation," J. Appl. Physiol., 28, 113-116, 1970.

73. Pierce, D. H., "A System for Measurement of Oxygen Consumption and the Control of Inspired Carbon Dioxide," IEEE Trans., BME-16, 235-237, 1971.

74. Folgering, H. th., Bernards, J. A., Sistermans, J. F. and Michels, B., "Automatic stabilization of inspiratory oxygen pressure and end expiratory carbon dioxide pressure in a closed spirometer system," Phlugers Arch., 347, 351-357, 1974.

75. Bellville, J. W., Fleischli, G. and Attura, G., "Servo Control of Inhaled Carbon Dioxide," J. Appl. Physiol., 24, 414-415, 1968.

76. Lambertsen, C. J. and Wendel, H., "An Alveolar pCO_2 Control System: Its Use to Magnify Depression by Meperidine," J. Appl. Physiol., 15, 43-48, 1960.

77. Stoll, P. J., Estavillo, J. A., Osborne, J. L. and Burger, R. S., "Control Theory Applied to the Chemical Regulation of Breathing," Buckles, R. G., Advances in Bioengineering, Chemical Engineering Progress Symposium Series 114, 67, 202-210, 1971.

78. Jain, V. K. and Guha, S. K., "A Study of Intermittent Positive Pressure Ventilation," Med. and Biol. Engng., 8, 575-583, 1970.

79. Holloman, Jr., J. H., Milhorn, Jr., H. T. and Coleman, T. G., "A Sampled Data Regulator for Maintaining a Constant Alveolar CO_2," J. Appl. Physiol., 25, 463-468, 1968.

80. Hilberman, M., Schill, J. P. and Peters, R. M., "On-Line Digital Analysis of Respiratory Mechanics and the Automation of Respiratory Control," J. Thorac and Cardiov. Surg., 58, 821-828, 1969.

81. Mitamura, Y., Mikami, T., Sugawara, H. and Yoshimoto, C., "An Optimally Controlled Respirator," IEEE Trans., BME-18, 330-337, 1971.

82. Piiper, J. and Scheid, P., "Respiration: Alveolar Gas Exchange," Annual Review of Physiology, 7, 131-154, 1971.

83. Chilton, A. B. and Stacy, R. W., "A Mathematical Analysis of Carbon Dioxide Respiration in Man," Bulletin of Mathematical Biophysics, 14, 1 - 18, 1952.

84. Fung, Y. C., "Theoretical Pulmonary microvascular Impedance," Annals of BioMedical Engineering, 1, 221-245, 1972.

85. Wolstenholme, G. E. W. and Knight, J. (eds.), Circulatory and Respiratory Mass Transport, Little, Brown and Company, Boston, 1969.

86. Fowler, K. T. and Read, J., "Cardiac Oscillations in expired gas tensions and regional pulmonary blood flow," J. Appl. Physiol, 16, 863-868, 1961.

87. Sikand, R., Ceretelli, P. and Farhi, L. E., "Effects of $\dot{V}_A$ and $\dot{V}_A/\dot{Q}$ distribution and of time on the alveolar plateau," J. Appl. Physiol., 21, 1331-1337, 1966.

88. Trimble, D., Smith, D., Rosenthal, M. and Fosberg, R., "Carbon Dioxide Supplementation as a Therapeutic Adjunct in Post-Traumatic Pulmonary Insufficiency," Southwestern Surgical Congress, 1971.

89. Flumerfelt, R. W. and Crandall, E. D., "An Analysis of External Respiration in Man," Mathematical Biosci., 8, 205-230, 1968.

90. Wagner, P. D. and West, J. B., "Effects of Diffusion Impairment on O_2 and CO_2 Time Courses in Pulmonary Capillaries," J. Appl. Physiol., 33, 62-71, 1972.

91. Suwa, K. and Bendixen, H. H., "A Mathematical Analysis of Physiological Deadspace in a Lung Model," J. Appl. Physiol., 24, 549-555, 1968.

92. Suwa, K, and Bendixen, H. H., "Change in P_ACO_2 with Mechanical Deadspace During Artificial Ventilation," J. Appl. Physiol., 24, 556-563, 1968.

93. Suwa, K., Geffin, B., Pontoppidan, H. and Bendixen, H. H., "A nomograph for deadspace requirement during prolonged ventilation," Anesthesiology, 29, 1206-1210, 1968.

94. Crossman, P. F., Bushnell, L. S. and Hedley-White, J., "Deadspace During Artificial Ventilation: Gas Compression and Mechanical Deadspace," J. Appl. Physiol., 28, 94-97, 1970.

95. Farhi, L. E. and Rahn, H., "Gas Stores in the Body and the Unsteady State," J. Appl. Physiol., 7, 472-484, 1955.

96. Farhi, L. E. and Rahn, H., "Dynamic Changes in Carbon Dioxide Stores," Anesthesiology, 21, 604-614, 1960.

97. Farhi, L. E., "Gas Stores of the Body," Fenn, W. O. and Rahn, H. (eds.), Hnbk of Physiol., Sec III, Respiration, 1, American Physiological Soc., Washington, D.C., 1964.

98. Cherniack, N. S., Longobardo, G. S., Staw, I. and Heymann, M., "Dynamics of Carbon Dioxide Changes Following and Alteration in Ventilation," J. Appl. Physiol., 21, 785-793, 1966.

99. Cherniack, N. S., Longobardo, G. S., Palermo, F. P. and Heymann, M., "Dynamics of Oxygen Stores Changes Following an Alternation in Ventilation," J. Appl. Physiol., 24, 809-816, 1968.

100. Cherniack, N. S., and Longobardo, G. S., "Oxygen and Carbon Dioxide Gas Stores of the Body," Physiol. Rev., 2, 196-243, 1970.

101. Bates, D. V., Macklem, P. T. and Christie, R. V., Respiratory Function in Disease, Saunders, Philadelphia, 1971.

102. Slonim, N. B., Bell, B. P. and Christensen, S. E., Cardiopulmonary Laboratory Basic Methods and Calculations, Thomas, Springfield, Illinois, 1967.

103. Stacy, R. W. and Peters, R. M., "Computations of Respiratory Mechanical Parameters," in Stacy, R. W. and Waxman, B. H., Advances in Biomedical Computers, II, Wiley, 1966.

104. Finucane, K. E., Egan, B. A. and Dawson, S. V., "Linearity and Frequency Response of Pneumotachographs," J. Appl. Physiol., 32, 121-126, 1972.

105. Turney, S. Z. and Blumenfeld, W., "Heated Fleisch pneumotachometers: Calibration procedure," J. Appl. Physiol., 34, 117-118, 1973.

106. Puryear, G. H., Osborn, J. J., Beaumont, J. O. and Gerbode, F., "The Influence of Adjuvant Ventilators in the Respiratory Effect of Accutely Ill Patients," Annals of Surgery, 170, 900-909, 1969.

107. Jackovitch, T. and Eberhart, R. W., "The Doppler Principle Applied to Respiratory Flow Measurement," Proc. of San Diego Biomedical Symposium, 12, 47-52, 1972.

108. Turney, S. Z. and Blumenfeld, W., "Ultrasonic spirometer: A calibration procedure," Med. Biol. Eng., 9, 292-294, 1974.

109. General Electric Company, "Proposal for Development of Production Prototype of a Portable Volume Controlled Respiratory," 1 October 1971.

110. Bouton, B. W., "Measurement of Inspired and Expired Oxygen and Carbon Dioxide," Brit. J. Anaesthesia, 41, 723-730, 1969.

111. Fowler, K. T., "The Respiratory Mass Spectrometer," Phys. Med. Biol., 14, 185-199, 1969.

112. Kleiman, B. S., Brantigan, O. and Zapata, A., "On-line O_2 and CO_2 Analysis in Vivo," J. Assn. Advan. Med. Instrum., 5, 224-226, 1971.

113. Woldring, S., "Biomedical Application of Mass Spectrograph for Monitoring Partial Pressures, A Technical Review," J. Assn. Advan. Med. Instrum., 4, 43-56, 1970.

114. Wald, A., Has, W. K. and Ransohoff, J., "Experience with a Mass Spectrometer System for Blood Gas Analysis in Humans," J. Assn. Advan. Med. Instrum., 5, 325-342, 1971.

115. Turney, S. Z., Blumenfeld, W., "On-line Respiratory Waveform Analysis Using a Desk Calculator," Med. Biol. Eng., 8, 320-331, 1973.

116. Buzza, E. E., Leonard, J. E., Watanabe, H. and Carlsen, E. N., "A New Electrode System for Continuous Measurement of pH, PCO_2, PO_2 and Temperature on Flowing Blood," J. Assn. Advan. Med. Instrum., 4, 136-144, 1970.

117. Johnson, C. C., Palm, E. D., Stewart, D. C. and Martin, W. E., "A Solid State Fiberoptics Oximeter," J. Assn. Advan. Med. Instrum., 5, 77-83, 1971.

118. Lopez-Majano, V., Alfredson, K. S., Cumas, W. and Kearns, K., "Evaluation of Light Reflection Oximeter," Amer. J. Clin. Pathol., 55, 701-704, 1970.

119. Turney, S. Z., McAslan, T., Crawford, C. and Adams, R., "The Continuous Measurement of Pulmonary Gas Exchange and Mechanics," Annals of Thoracic Surgery, 11, 229-242, 1972.

120. Dennis, M. W., Douglas, J. S., Casby, J. U., Stolwijk, J. A. J. and Bouhuys, A., "On-Line Analog Computer for Dynamic Lung Compliance and Pulmonary Resistance," J. Appl. Physiol., 26, 248-252, 1969.

121. Hyatt, R. E., Zimmerman, I. R., Peters, G. M. and Sullivan, W. J., "Direct Writeout of Total Respiratory Resistance," J. Appl. Physiol., 28, 675-678, 1970.

122. Neeley, W. A., Robinson, W. T., Holloman, Jr., G. H. and McMullan, M. H., "An Inexpensive Bedside Analogue Computer for Measuring Respiratory Work and Certain Other Parameters," Surgery, 69, 309-313, 1969.

123. Peters, R. M. and Stacy, R. W., "Automatized Clinical Measurement of Respiratory Parameters," Surgery, 56, 44-52, 1964.

124. Uhl, R. R. and Lewis, F. J., "Digital computer calculation of human pulmonary mechanics using a least squares fit technique," Computers and Biomedical Research, 7, 489-495, 1974.

125. Roy, R., Powers, Jr., S. R. and Kimball, W. R., "Estimation of respiratory parameters by the method of covariance rations," Computers and Biomedical Research, 7, 21-39, 1974.

126. Van Bergen, F. H., Novak, A. L. and Cumming, J. F., "Analog Computer for On-Line Determinations of Ventilatory Power, Work and Volume," Medical Research Engineering, 5, 7-13, 1970.

127. Cook, C. D., Sutherland, J. M., Segal, S., Cherry, R. B., Mead, J., McIlroy, M. B. and Smith, C. A., "Studies of Respiratory Physiology in the New Born Infant — III, Measurements of Respiration," J. Clin. Invest., 36, 440-448, 1957.

128. Osborne, J. J., Raison, J. C. A., Beaumont, J. O., Hill, J. D., Kerth, W. J., Popper, R. W. and Gerbode, F., "Respiratory Causes of 'Sudden Unexplained Arrhythmias' in Postthoractomy Patients," Surgery, 69, 24-28, 1971.

129. Ruttiman, U. E. and Yamamoto, W. S., "Quantitation of ventilation in terms of continuous airflow variables," Computers in Biomedical Research, 8, 239-251, 1974.

130. Mohler, R. R., "Natural Bilinear Control Processes," IEEE Trans., SCC-6, 192-197, 1970.

131. Mohler, R. R. and Smith, W. D., "Foundations of Bilinear Compartmented Physiological Systems," Proc. Southwestern IEEE Conf. Rec., 22, 157-160, 1970.

132. Mohler, R. R. and Rink, R. E., "Completely Controllable Bilinear Systems," SIAM J. Control, 6, 477-486, 1968.

133. Mohler, R. R. and Rink, R. E., "Control with a Multiplicative Mode," J. Basic Engng., 30, 201-206, 1969.

134. Mohler, R. R. and Rink, R. E., "Reachable Zones for Equicontinuous Bilinear Control Processes," Int. J. Control, 14, 331-339, 1971.

135. Pontryagin, L. S., Boltyanskii, V. G., Gamkrelidze, R. V. and Mischenko, E. F., The Mathematical Theory of Optimal Processes, Wiley-Interscience, New York, 1962.

136. Athans, M. and Falb, P. L., Optimal Control, McGraw-Hill, New York, 1966.

137. Ryan, E. P., "Time-optimal Feedback Control Laws for Certain Third-Order Relay Control Systems," Int. J. Control, 20, 881-911, 1974.

138. Luenberger, D. G., Introduction to Linear and Nonlinear Programming, Addison-Wesley, Reading, Mass., 1973.

139. Potter, J. E., "Matrix Quadratic Solutions," J. SIAM Appl. Math., 14, 496-501, 1966.

140. Kuo, B. C., Discrete-Data Control Systems, Prentice-Hall, 1970.

141. Rozonoer, L. I., "The Maximum Principle of L. S. Pontryagin in Optimal System Theory," Parts I, II, III, Automation and Remote Control, 20, 1959.

142. Utkin, V. I., "Variable Structure Systems," Lecture Notes, University of Illinois, Urbana, Illinois, 1975.

143. Moon, S. F., "Optimal Control of Bilinear Systems and Systems Linear in Control," Ph.D. Dissertation, Electrical Engineering Department, University of New Mexico, Santa Fe, New Mexico, 1969.

144. Singh, G., "Optimization and Decoupling of Large Dynamic Systems with Applications to Power Systems," Ph.D. Dissertation, Electrical Engineering Department, University of Illinois, Urbana, Illinois, 1972.

145. Folkerts, C. H., "Nonlinear Magnetic Circuit Analysis of a Step Motor," M.S. Thesis, Electrical Engineering Department, University of Illinois, Urbana, Illinois, 1975.

146. Hilberman, M., Komm, B., Tarter, M. and Osborne, J. J., "An Evaluation of Computer Based Patient Monitoring at Pacific Medical Center," Computers in Biomedical Research, 8, 447-460, 1975.

APPENDIX A

SIMILARITY TRANSFORMATION DERIVATION

The similarity transform is used to diagonalize a linear set of simultaneous differential equations like those in vector representation below

$$\dot{\underline{x}} = A_{3L}\underline{x} + B_{3L} \quad .$$

The eigenvectors of A_{3L} are used to calculate the similarity transform. The eigenvectors come from the following relation:

$$(\lambda_i I - A_{3L})\ \underline{x}_i = 0 \qquad \text{(A-1)}$$

where

$$\lambda_i = 0, \lambda_1, \lambda_2$$

$\underline{x}_i$ is the ith eigenvector .

From the above relationship we get three simultaneous equations

$$\lambda_i x_3 = 0 \quad \text{so } x_3 = \alpha_0 \qquad \text{for } \lambda_i = 0$$

$$= 0 \qquad \text{for } \lambda_i \neq 0 \qquad \text{(A-2)}$$

$$x_1 = \frac{(\lambda_i + a_{21})}{a_{21}}\, x_2 \qquad \text{(A-3)}$$

and

$$x_1 = \left(\frac{a_{12}}{x_1 + a_{12} + b_1 y_{3e}}\right) x_2 - \left(\frac{b_1 y_{1E}}{\lambda_i + a_{12} + b_1 y_{3e}}\right) x_3 \quad . \qquad \text{(A-4)}$$

Equating x_1 in Eq. (A-3) and (A-4), we obtain

$$x_2 = \frac{-b_1 y_{1e} a_{21}}{\lambda_i^2 + (a_{12} + a_{21} + b_1 y_{3e})\lambda_i + b_1 y_{3e} a_{21}} x_3 \quad . \tag{A-5}$$

For $\lambda_i = 0 = \lambda_0$

$$\underline{x}_0 = \begin{vmatrix} \frac{-y_{1e}}{y_{3e}} \\ \\ \frac{-y_{1e}}{y_{3e}} \\ \\ 1 \end{vmatrix} \alpha_0 \quad . \tag{A-6}$$

Normalizing the eigenvector $\underline{x}_0 = [x_{10}, x_{20}, x_{30}]^T$ so that the vector's elements satisfy the following relationship

$$\sum_{i=1}^{3} x_{i0}^2 = 1 \tag{A-7}$$

we see that

$$\alpha_0 = \sqrt{\frac{1}{1 + 2\left[\frac{y_{1e}}{y_{3e}}\right]^2}} \quad . \tag{A-8}$$

If $\lambda_i \neq 0$ the denominator must equal zero since it is the product nonzero root factors of the characteristic equation. Therefore, Eq. (A-5) must be modified. Equating (A-3) and (A-4), but not solving for x_2, we obtain

$$\left(\frac{\lambda_i^2 + (a_{12} + b_1 y_{3e} + a_{31})\,\lambda_i + a_{21} b_1 y_{3e}}{(\lambda_i + a_{12} + b_1 y_{3e})\,a_{21}}\right) x_2 = \left(\frac{b_1 y_{1e}}{\lambda_1 + a_{12} + b_1 y_3}\right) x_3 \quad . \tag{A-9}$$

Since the numerator of the right-hand size is zero for $x_i \neq 0, x_3 = 0$ for $x_i \neq 0$. Therefore, x_2 must be an arbitrary constant $\alpha_i (i = 1,2)$, so

$$x_1 = \begin{vmatrix} \dfrac{\lambda_i + a_{21}}{a_{21}} \\ 1 \\ 0 \end{vmatrix} \alpha_i \qquad i = 1,2 \quad . \tag{A-10}$$

Normalizing and solving for α_i, we get

$$\alpha_i = \sqrt{\frac{1}{1 + \left(\dfrac{\lambda_i + a_{21}}{a_{21}}\right)^2}} \tag{A-11}$$

so the similarity transformation S

$$S = \begin{vmatrix} S_{11} & S_{12} & S_{13} \\ S_{21} & S_{22} & S_{23} \\ S_{31} & S_{32} & S_{33} \end{vmatrix}$$

where

$$S_{11} = S_{21} = \frac{-y_1}{y_3}\alpha_0 \tag{A-12a}$$

$$S_{31} = \alpha_0 \tag{A-12b}$$

$$S_{12} = \frac{\lambda_1 + a_{21}}{a_{21}} \quad , \quad S_{22} = S_{12}a_1 \tag{A-12c}$$

$$S_{13} = \frac{\lambda_2 + a_{21}}{a_{21}} \quad , \quad S_{23} = S_{13}\alpha_2 \tag{A-12d}$$

$$S_{32} = S_{33} = 0 \quad . \tag{A-12e}$$

Hence,

$$|S| = \frac{\alpha_0\alpha_1\alpha_2(\lambda_1 - \lambda_2)}{a_{21}} \tag{A-13}$$

$$S^{-1} = \frac{\begin{vmatrix} 0 & S_{31}S_{23} & -(S_{22}S_{31}) \\ 0 & -S_{31}S_{13} & S_{31}S_{12} \\ \frac{|S|}{\alpha_0} & -(S_{11}S_{23} + S_{21}S_{13}) & (S_{11}S_{22} - S_{12}S_{21}) \end{vmatrix}}{|S|} \quad . \tag{A-14}$$

The diagonalized A is

$$\Lambda = S^{-1}A_{3L}S \tag{A-15}$$

$$\Gamma = S^{-1}B_{3L} = B_1\left[1,\ \frac{\lambda_1 + a_{21}}{a_{21}},\ -\frac{\lambda_1}{a_{21}}\right]^T \tag{A-16a}$$

$$= \begin{vmatrix} \frac{\eta}{\alpha_0} \\ \frac{y_1 e^{\eta\lambda_2}}{y_3 e^{\alpha_1}(\lambda_1 - \lambda_2)} \\ \frac{y_1 e^{\eta\lambda_1}}{y_3 e^{\alpha_2}(\lambda_1 - \lambda_2)} \end{vmatrix} . \tag{A-16b}$$

APPENDIX B

COMPUTER PROGRAMS

This appendix contains some of the programs used to do the calculations for this dissertation. These programs represent the less straight forward approaches not obvious from the text.

B.1 Time Optimal Continuous Control Calculation

CONTROL1 implements the control law described in Section 3.2.1. It compensates for overflow, underflow and negative logrithms. It is called from the routine using the control law. The transformation of Eq. (3-23) from $\underline{x}$ to $\underline{v}$ is represented by the E matrix using $\underline{y}$ instead of $\underline{x}$.

```
      SUBROUTINE CNTRL1(Y,IPRINT)
C     ***************************************************************
C
C
      DIMENSION Y(6),DERY(6),PRMT(5)
      DIMENSION X1(250),X2(250),X3(250),X1DOT(250),X2DOT(250)
      COMMON J,OUTDEL,DELT,A21,A12,R1,Y1E,Y3E,ETA,E11,E12,E13,E21,E22,
     1E23,E31,E32,E33,SMALLA,XL1,XL2,U,X1,X1DOT,X2,X2DOT,X3
      E=2.7182818
      DATA EXPMIN,EXPMAX/-37.,37./
C
      IPRINT=IPRINT+1
C
C     CALCULATE V COORDINATES
C
      V1=E11*Y(1)+E12*Y(2)+E13*Y(3)
      V2=E21*Y(1)+E22*Y(2)+E23*Y(3)
      V3=E31*Y(1)+E32*Y(2)+E33*Y(3)
      IF(IPRINT-1)200,201,200
201   PRINT 299,V1,V2,V3,(Y(I),I=1,3)
      PRINT 301,E11,E12,E13,E21,E22,E23,E31,E32,E33,SMALLA
299   FORMAT(4H V1=,F12.5,4H V2=,E12.5,4H V3=,F12.5,7H Y(I)=,3(E12.5,1X
     1)
301   FORMAT(5H E11=,E12.5,5H E12=,E12.5,5H E13=,E12.5/,5H E21=,E12.5,
     1 5H E22=,E12.5,5H E23=,E12.5/,5H E31=,E12.5,5H E32=,E12.5,5H E33=
     2 E12.5/,8H SMALLA=,E12.5//)
200   CONTINUE
```

```
C
C       CALCULATE G
C
        G=-SMALLA*XL2*(XL2*V2+V3)
        SIGNG=TSIGN(G)
        IF(IPRINT-1) 202,203,202
203     PRINT 298,G,SIGNG
298     FORMAT(3H G=,E12.5,2X,F12.5)
202     CONTINUE
C
C       CALCULATE SIGMA(V2,V3)
C
        SIGMA=V3+SIGNG/XL2/SMALLA*ALOG(1.+ABS(G))
        SSIGMA=TSIGN(SIGMA)
        IF(IPRINT-1) 204,205,204
205     PRINT 297,SIGMA,SSIGMA
297     FORMAT(7H SIGMA=,E12.5,2X,F12.5)
204     CONTINUE
C
C       CALCULATE H
        T1=1.
        T2=1.+G*SSIGMA
        T3=SMALLA*XL2*V3*SSIGMA
        CALL PRODCH(T1,T2,T3,T4,TEM,IFIX)
        IF(IFIX-1) 100,101,100
C
C       SEE IF FIXED UP ON OVERFLOW
C
101     CONTINUE
C
C       YES,SEE IF CAN USE MAX VALUE AND REMAIN WITHIN BOUND DUE TO SQRT
C
        IF(TEM-EXPMAX-EXPMAX) 106,100,100
C
C       YES CAN FIX UP
C
106     CONTINUE
        T5=10.**(TEM/2.)
        IF(IPRINT-1)206,207,206
296      FORMAT(4H T1=,E12.5,4H T2=,E12.5,4H T3=,E12.5,4H T4=,E12.5,5H TE
      1,E12.5,6H IFIX=,I2)
207      PRINT 296,T1,T2,T3,T4,TEM,IFIX
206     CONTINUE
        T4SIGN=TSIGN(T4)
        T4=T5*T4SIGN
C       NOW CHECK UP ON SQRT ARGUMENT SIGN
C
C
100     CONTINUE
        IF(1.-T4) 104,105,105
C
C         BAD SQRT:IMAGINARY
C
104     PRINT 107
107     FORMAT(14H NEG SQRT OF H  )
        U=0.
        RETURN
```

```
105     H=1.+SQRT(1.-T4)
C
C       CALCULATE PHI
C
          T1=XL1/XL2*LOG10(H)
          IF(T1-EXPMAX) 150,150,151
151       T1=EXPMAX
          GO TO 152
150       T1=H*(XL1/XL2)
152       CONTINUE
        T2=2.-T1
        T3=-XL1*SMALLA*V3*SSIGMA
        T5=XL1-XL2
          CALL PRODCH(T1,T2,T3,XPROD,TEM,IFIX)
        PHI=V1*(V2+(V3+SSIGMA/SMALLA/XL1*XPROD)/XL1)/T5
C
C       PERFROM THE CONTROL LAW
C
        IF(ABS(PHI)-1.E-10) 21,21,20
21      U= SSIGMA
        RETURN
20      U= TSIGN(PHI)
        RETURN
        END
        SUBROUTINE PRODCH(T1,T2,T3,T4,TEM,IFIX)
C
C       BOUNDING CONSTANTS
C
        EMAX=72.
        EXPMIN=-72.
        E=2.71828183
        XLOGE=.4342945
        EXPMAX=EMAX/XLOGE
        IFIX=0
C
C       CHECK LOG AND SIGN OF T1
C
        CALL XLOGT(T1,SIGNT1,XLOGT1)
        IF(SIGNT1)   1,100,1
1       CONTINUE
C
C       CHECK SIGN AND LOG OF T2
C
        CALL XLOGT(T2,SIGNT2,XLOGT2)
        IF(SIGNT2) 2,99,2
C
C
2       CONTINUE
        SIGNT=SIGNT1*SIGNT2
        IF(T3) 3,34,5
C
C       LESS THAN ZERO*CHECK FOR UNDERFLOW
3       CONTINUE
        IF(T3-EXPMIN)33,33,34
C       CHECK EXPONENT T3
```

```
C
C       UNDERFLOW' FIX UP
33      T5=EXPMIN
        GO TO 10
34      T5=T3
        GO TO 10
C
C       CHECK FOR EXPONENT OVERFLOW
C
5       CONTINUE
        TEM=T3*XLOGE
        IF(TEM-EXPMAX) 34,51,51
C
C       OVERFLOW' FIX UP
C
51      T5=EXPMAX
C
C       SEE IF PRODUCT T1*T2*E**T3 OVER/UNDERFLOW
C
10      CONTINUE
        TEM=XLOGT1+XLOGT2
        ATEM=ABS(TEM)
        IF(ATEM-EXPMAX) 6,6,61
C
C       OVER/UNDERFLOW FIXUP
C
61      TEM=TEM/ATEM*EXPMAX
6       CONTINUE
        TEM=TEM+T5*XLOGE
C
C       CHECK ON PRODUCT
C
        IF(TEM-EMAX)161,62,62
161     IF(TEM-EXPMIN) 63,63,64
C
C       OVERFLOW FIXUP
62      T4=SIGNT*10.**EMAX
65      IFIX=1
        RETURN
C
C       UNDERFLOW FIXUP
C
63      T4=SIGNT*10.**EXPMIN
        GO TO 65
C
C       OK IN RANGE,CALCULATE VALUE
64      T4=T1*T2*E**(T3)
        RETURN
C       X1=0\ T4=0(TEM=0,IFIX=2
100     CONTINUE
C       X2=0\ T4=0,TEM=0,IFIX=2
99      CONTINUE
        T4=0.
        TEM=0.
        IFIX=2
```

```
      RETURN
      END
      SUBROUTINE XLOGT(T3,SIGNT3,XLOGT3)
C
C     SUBROUTINE TO TEST OVER AND UNDERFLOW BEFORE EXPONENTIATION
C
C
C
C     SIGNT3=1 IF LOG(T3)>, =-1 IF LOG(T3)<0, =0 IF T3=0
C
C
      SIGNT3=1.
      IF(T3)30,31,32
30    SIGNT3=-1.
32    T4=ABS(T3)
      IF(T4-1.)33,34,35
33    XLOGT3=-ALOG10(T4)
      RETURN
35    XLOGT3=ALOG10(T4)
31    SIGNT3=0.
34    XLOGT3=0.
      RETURN
      END
```

B.2 Ricatti Solution Using the Eigenvector Method of Potter

This program is based upon Singh's [144] implementation of the eigenvector method of Potter. It uses the standard matrix routines from IBM Scientific Subroutine Package as well as two special subroutines from the EISPAK eigenvalue package developed by Argonne Laboratory. These two special routines are EIGENP for general matrix eigenvalues and EIGENZ for real symmetric matrix eigenvalues.

```
      DIMENSION A(3,3),B(3,1),Q(3,3),R(1,1),AA(3,3),G0(1,3)
      DIMENSION ROOTR(6),ROOTI(6),INDEX(6)
      DIMENSION GAINS(40,3),EIGENR(40,3),TITLE(40,2),T(2)
      REAL*8 A,B,Q,R,AA,G0,ROOTR,ROOTI
      M=1
        CALL ASSIGN(5,'RIKENG.DAT;1',12)
        CALL ERRSET(81,,TRUE.,,FALSE.,,FALSE.,,FALSE.,,999)
      N=3
      N2=N*2
      IPASS=1
      IPRINT=1
1     CALL DATA(A,B,Q,R,T,N,M,IDONE)
      IF(IDONE.EQ.1) GO TO 100
      CALL RICOTI(A,B,Q,R,AA,G0,ROOTR,ROOTI,INDEX,N,N2,M,IGOOD,IPRINT)
      IPASS=IPASS+1
      IF(IGOOD.NE.0) GO TO 20
      DO 10 I=1,N
      GAINS(IPASS,I)=G0(1,I)
      EIGENR(IPASS,I)=ROOTR(I)
      IF(I.GE.3) GO TO 10
      TITLE(IPASS,I)=T(I)
10    CONTINUE
      GO TO 1
20    IPASS=IPASS-1
      GO TO 1
100   PRINT 102
```

```
102   FORMAT(1H1,' RICOTTI GAINS COMPARISON',/,1H ,'VARIATION',2X,'X(1)
     1GAIN',4X,'X(2) GAIN',4X,'X(3) GAIN')
        CALL BUBBLE(EIGENR,N,IPASS)
        CALL BUBBLE(GAINS,N,IPASS)
      DO 200 I=1,IPASS
200   PRINT 101,  (TITLE(I,J),J=1,2),(GAINS(I,J),J=1,N)
101   FORMAT(1H ,2X,2A4,1P9E13.5)
      PRINT 103
103   FORMAT(1H1,' (A-SP) EIGENVALUE COMPARISON',/,1H ,2X,2A4,'VARIATION
     1',2X,'X(1)E VALUE X(2)E VALUE X(3)E VALUE')
      DO 201 I=1,IPASS
201   PRINT 101,  (TITLE(I,J),J=1,2),(EIGENR(I,J),J=1,N)
      STOP
        CALL CLOSE (5)
      END
        SUBROUTINE BUBBLE(A,M,N)
        DIMENSION A(40,3)
        DO 100 I=1,N
        DO 90 J=1,M
        DO 90 K=J,M
        IF (A(I,K).GE.A(I,J))GO TO 90
        TEM=A(I,K)
        A(I,K)=A(I,J)
        A(I,J)=TEM
90      CONTINUE
100     CONTINUE
        RETURN
        END
        SUBROUTINE RICOTT(A,B,Q,R,AA,G0,ROOTR,ROOTI,INDEX,N,N2,M,IGOOD,
     1IPRINT)
C
C     ***************************************************************************
C               EIGENVECTOR METHOD FOR SOLVING A NNNTH ORDER ALGEBRAIC
C               RICCATI EQUATION
C     ***************************************************************************
C
C
C     **********     INPUT VARIABLES   ***********************************
C
C     A       THE SYSTEM MATRIX
C
C     B       THE CONTROL INPUT MATRIX
C     R       THE INVERSE OF THE CONTROL WEIGHTING MATRIX
C
C     Q       THE STATE WEIGHTING MATRIX
C
C     N       IS THE DIMENSION OF THE STATE VARIABLE VECTOR
C
C     N2      =2*N
C
C     M       IS THE DIMENSION OF THE CONTROL VECTOR
C
C     IPRINT =0,NO PRINTOUT;=1,PRINT OUT IMPORTANT VALUES;=2,PRINT ALL
C
C     **********     OUTPUT VARIABLES     ************************************
C
C
```

```
C       AA      CONTAINS THE RESULT OF A-SP
C
C       G0      CONTAINS THE CALCULATED  STATE VARIABLE FEED BACK GAINS FOR
C               THE CONTROL U
C
C       ROOTR   REAL PARTS OF THE EIGENVALUES OF THE MATRIX (A-SP)
C
C       ROOTI   IMAGINARY PARTS OF THE EIGEN VALUES OF THE MATRIX (A-SP)
C
C       INDEX   =2;IF EIGENVALUES ARE GOOD-OUTPUT FROM EIGENP,EIGENZ
C
C       IGOOD   ZERO,, IF NO PROBLEM IN SUBROUTINE RICOTI
C
        DIMENSION A(3,3),S(3,3),Q(3,3),TL(3,3),TS(3,3),WORK(3,3),P(3,3),
       1Z(3),BIGM(6,6),VECR(6,6),VECI(6,6),ROOTR(6),ROOTI(6),INDEX(6),
       2LW(3),NW(3),CONE(6,3),AA(3,3),B(3,1),R(1,1),BT(1,3),G0(1,3),ROOT(6
       3),AAA(3,3)
        DOUBLE PRECISION A,S,Q,TL,TS,WORK,P,BIGM,VECR,VECI,ROOTR,ROOTI,AA,
       1CONE,DT,B,R,BT,G0,ROOT,AAA
        CALL ERRSET(208,256,5,1)
        PRINT 117
117     FORMAT(//)
C
C                                T -1
C       CALCULATE S MATRIX,B R   B
C
        CALL GMPRD(B,R,TL,N,M,M)
        CALL GMTRA(B,BT,N,M)
        CALL GMPRD(TL,BT,S,N,M,N)
C
C       PRINT INPUT MATRICES FOR EIGENVECTOR METHOD
C
        IF(IPRINT.LT.1) GO TO 300
        PRINT 104
104     FORMAT(/4X,'THE A MATRIX')
        CALL GPRINT(A,N,N)
        PRINT 107
107     FORMAT(/4X,'THE B MATRIX')
        CALL GPRINT(B,N,M)
        PRINT 105
105     FORMAT(/4X,'THE Q MATRIX')
        CALL GPRINT(Q,N,N)
        PRINT 114
114     FORMAT(/4X,'THE R-INVERSE MATRIX')
        CALL GPRINT(R,M,M)
        PRINT 106
106     FORMAT(/4X,'THE S MATRIX')
        CALL GPRINT(S,N,N)
C
C       FORM THE BIG MATRIX 2NX2N
C
300     DO 3 I=1,N
        DO 3 J=1,N
        AA(I,J)=A(I,J)
        BIGM(I,J)=A(I,J)
```

```
      BIGM(I+N,J+N)=-A(J,I)
      BIGM(I,J+N)=-S(I,J)
3     BIGM(I+N,J)=-Q(I,J)
      CALL EIGENP(N, N,AA,ROOTR,ROOTI,TL,TS,INDEX)
      IF(IPRINT.LT.1) GO TO 210
      PRINT 102
102   FORMAT(/4X,'EIGENVALUES OF THE A-MATRIX')
      PRINT 101
      DO 21 I=1,N
21    PRINT 200,I,ROOTR(I),ROOTI(I),INDEX(I)
210   CONTINUE
      CALL EIGENP(N2,N2,BIGM,ROOTR,ROOTI,VECR,VECI,INDEX)
      IF(IPRINT.LT.2) GO TO 400
      PRINT 100
100   FORMAT(/4X,'EIGENVALUES OF THE BIG M MATRIX')
      PRINT 101
      DO 4 I=1,N2
4      PRINT 200,I,ROOTR(I),ROOTI(I),INDEX(I)
400   MM=0
      I=1
16    IF(I-N2) 17,17,18
17    IF(ROOTR(I)) 8,15,7
8     MM=MM+1
      IF(ROOTI(I))9,10,9
10    DO 11 J=1,N2
11    CONE(J,MM)=VECR(J,I)
      GO TO 7
9     I=I+1
      DO 13 J=1,N2
      CONE(J,MM)=VECR(J,I)
13    CONE(J,MM+1)=VECI(J,I)
      MM=MM+1
7     I=I+1
      GO TO 16
18    CONTINUE
      DO 14 I=1,N
      DO 14 J=1,N
      TS(I,J)=CONE(I,J)
14    TL(I,J)=CONE(I+N,J)
      CALL MINV (TS,N,DT,LW,NW)
      IF(IPRINT.GE.1) PRINT 116,DT
116   FORMAT(/'     DET=',1PE12.5)
      CALL GMPRD(TL,TS,P,N,N,N)
      CALL GMPRD(S,P,TL,N,N,N)
      CALL GMSUB(A,TL,AA,N,N)
      CALL GTPRD(B,P,BT,N,M,N)
      CALL GMPRD(R,BT,G0,M,M,N)
      CALL EIGENZ(P,TL,ROOT,TS,N,N,1)
      DO 1000 J1=1,N
      DO 1000 J2=1,N
1000  AAA(J1,J2)=AA(J1,J2)
      CALL EIGENP(N,N,AAA,ROOTR,ROOTI,TL,TS,INDEX)
      IF(IPRINT.LT.1) GO TO 1100
      PRINT 110
110   FORMAT(/4X,'THE RICCATI GAINS')
      CALL GPRINT(P,N,N)
```

```
      PRINT 112
112   FORMAT(/4X,'THE A-SP MATRIX')
      CALL GPRINT(AA,N,N)
      PRINT 115
115   FORMAT(/4X,'THE FEEDBACK GAINS')
      CALL GPRINT(G0,M,N)
      PRINT 113
113   FORMAT(/4X,'EIGENVALUES OF THE RICCATI MATRIX')
      PRINT 111,(ROOT(I),I=1,N)
      PRINT 103
103   FORMAT(/4X,'EIGENVALUES OF A-SP')
      PRINT 101
      DO 22 I=1,N
22    PRINT 200,I,ROOTR(I),ROOTI(I),INDEX(I)
      IF(IPRINT.LT.2) GO TO 1100
      PRINT 203
203   FORMAT(/4X,'EIGENVECTORS OF THE A-SP MATRIX')
      DO 24 I=1,N,3
      L=I+2
      IF(L.GT.N)L=N
      PRINT 202
      DO 24 J=1,N
      PRINT 111,(TL(J,K),TS(J,K),K=I,L)
24    CONTINUE
1100  IGOOD=0
      RETURN
101   FORMAT(4X,'ROOT NO',2X,'REAL PART OF ROOT',2X,
     1'IMAGINARY PART OF ROOT',2X,'INDEX')
108   FORMAT(4E20.8)
109   FORMAT(4E20.13)
111   FORMAT(2X,1P6E13.5)
200   FORMAT(6X,I2,8X,1PE12.5,8X,1PE12.5,9X,I2)
201   FORMAT(1P6E20.5)
202   FORMAT(4X,'REAL PART',4X,'IMAG PART',4X,'REAL PART',
     14X,'IMAG PART',4X,'REAL PART',4X,'IMAG PART')
501   FORMAT('1')
15    IGOOD=-1
      RETURN
      END
      SUBROUTINE DATA(A,B,Q,R,T,N,M,IDONE)
      REAL*8 A,B,Q,R
      DIMENSION A(N,N),B(N,N),Q(N,N),R(M,M),T(2)
      READ(5,111,END=99) C1,C2,R2,ETA,VC02,Y1E,(T(J),J=1,2)
111   FORMAT(6E10.3,10X,2A4)
      PRINT 200,C1,C2,R2,VC02,ETA,Y1E,(T(J),J=1,2)
200   FORMAT(1H1,4X,'C1=',E12.5,' C2=',E12.5,' R2=',E12.5,' VC02=',E12.5
     1,/,1H ,' ETA=',E12.5,' Y1E=',E12.5,' CHANGE IN ',2A4)
C
C     CALCULATED CONSTANTS
C
      A12=1./R2/C1
      A21=1./R2/C2
      Y3E=862.*VC02/Y1E
      B1=1./862./C1
C
C     CALCULATE A AND B  MATRICES
C
```

```
      A(1,1)=-(A12+B1*Y3E)
      A(1,2)=A12
      A(1,3)=-B1*Y1E
      A(2,1)=A21
      A(2,2)=-A21
      A(2,3)=0.
      A(3,1)=0.
      A(3,2)=0.
      A(3,3)=0.
      B(1,1)=0.
      B(2,1)=0.
      B(3,1)=ETA
C
C     PICK UP Q,MATRIX, UPPER TIRANGLE
C
      READ(5,1,END=99)((Q(I,J),J=I,N),I=1,N),((R(I,J),J=1,M),I=1,M)
1     FORMAT(7F10.3)
C
C     DEFINE LOWER TRIANGLE
      DO 6 I=1,N
      DO 6 J=1,I
6     Q(I,J)=Q(J,I)
      IDONE=0
      RETURN
99    IDONE=1
      RETURN
      END
```

B.3 Modified Newton Solution of Simultaneous Equations

This program is based upon the work of Folkerts [145]. It solves the equation

$$A\underline{x} = \underline{b}$$

for $\underline{x}$ using L-U decomposition. It needs an initial guess for $\underline{x}$ and avoids the inversion of A by the L-U decomposition. In addition to being used to solve the Ricatti equation, it can be used to solve the simultaneous transcendental equations of Section 3.4.

```
      SUBROUTINE NEWTON(XK,XK1,N,IRAD)
        IMPLICIT REAL*8(A-H,O-Z)
       DIMENSION XK(6),XK1(6),A(6,6),XK2(6),XKNEW(6),XKFI(6),IP(6),Q(3),
     1 XKINIT(6)
C
C       NORM@S
C       FKLAST = NORM OF F(X(K))
C       FKBEG  = NORM OF F(X(K-1))
C       XKNORM = NORM IF X(K)
C       XNORMF = NORM OF F(X(K+1))
C
C       K VECTORS
C
C       XK     = X(K)
C       XK1    = DEL OF (X(K+1)-X(K))
C       XKNEW  = X(K+1) CALCULATED
C
C       F(K) VECTORS
C
C       XKFL   = F(X(K))
C       XK2    = F(X(K+1))
C       SING CONSTANTS
C
C       IFIN   = 0 ; IF STILL SIZING EPSILN
C              = 1 ; IF EPSILN HAS BEEN PICKED
C
C       IDERIV = 0  ;
C              @
C              = 1 ; (F(X(K))-F(X(K+1))) IS NORM OF F DECREASING,
C                    ACCEPT PREVIOUS EPSILON
C
```

```
C
C       SET FOR NEWTON/RHAPSON EVLAUATION
C
C
C       EPSILN*A(,,,)*XK(K+1)-XK(K)) = F( X(K))
C
        IBAD=0
        INORM=1
830     CONTINUE
         FNMIN=1.E-4
         IPASS=0
         IFIN=0
         EPSILN=1.
        IPMAX=50
        CALL FEVLMP(XKFL,XK,XNORMF,1)
         FKLAST=XNORMF
         FKBE4=XNORMF
        DO 90 J1=1,N
90      XK1(J1)=XKFL(J1)
C
C        MAIN LOOP
C
100      IPASS=IPASS+1
        IF(IPASS-IPMAX) 101,101,801
101     CONTINUE
        IDECR=30
         IDERIV=0
C
C       EVLAUATE THE JACOBIAN MATRIX
C
         CALL JACOBI(XK,A)
        DO 778 L=1,N
778     PRINT 777, L,(A(L,M),M=1,N)
777     FORMAT(3H A(,I2,4H,X)=,6(E12.5,1X))
        CALL DECOMP(N,N,A,IP)
C
C        TEST FOR SINGULARITY OF A
C
         IF(IP(N)) 182,145,182
145     PRINT 146
146     FORMAT(1H ,20(1H*),18H SINGULAR SOLUTION    )
        GO TO 811
182     DO 183 L=1,N
183     XK1(L)=XK(L)
         CALL SOLVE(N,N,A,XK1,IP)
         DO 120 I1=1,N
120      XKINIT(I1)=XK1(I1)
C
C        INNER LOOP,DETERMINATION OF EPSILN
C
        IPRINT=0
110      CONTINUE
         XKNORM=0.
         DO 115 I2=1,N
         T1=XK(I2)-EPSILN*XK1(I2)
         XKNEW(I2)=T1
         XKNORM=XKNORM+T1*T1
```

```
115     CONTINUE
        IPRINT=IPRINT+1
        CALL FEVLMP(XK2,XKNEW,XNORMF,IPRINT)
111     FORMAT(7H XKNEW=,6(E12.5,1X))
112     FORMAT(7H NORMS=,3(E12.5,1X),3H F=,E12.5)
C
C       SEE IF NORM OF F(K) IS DECREASING
C
        IF(XNORMF-FKBEF4)  125,166,116
C
C      FIX FOR SATURATED NORM
166     IF(XNORMF-FKLAST) 130,128,117
C
116     IF(XNORMF-FKLAST)130,130,117
117     IF(IDERIV) 125,130,125
C
C       DECREASE EPSILN,NORM DECREASING IDERIV .NE. 0
C
130     FKLAST=XNORMF
        IDECR=IDECR-1
        IF(IDECR) 150,135,131
150     CONTINUE
        PRINT 151
151     FORMAT(36H UNABLE TO FIND EPSILON SMALL ENOUGH//)
        PRINT 152,((LL,XK2(LL)),LL=1,N)
152     FORMAT(3HF(,I2,2H)=,E12.5/)
        GO TO 800
131     EPSILN=EPSILN/2.
        PRINT 205
205     FORMAT(18H DECREMENT EPSILON  //)
        GO TO 110
C
C       SEE IF DECREASED EPSILN TOO MUCH
C
125     IF(XNORMF-FNMIN) 800,800,126
126     IF(IFIN-1) 127,135,127
127     IDERIV=1
        DELSIZ=XNORMF-FKLAST
        IF(DELSIZ) 130,128,128
C
C       SHRUNK EPSILN TOO MUCH,FINAL APPROXIMATION FOR EPSILN
C
128     CONTINUE
129     EPSILN=EPSILN+EPSILN
114     FORMAT(18H EPSILON PICKED,F=  ,E12.5)
        IFIN=1
        GO TO 110
C
C
C      ACCEPT EPSILN,SET UP FOR NEW PASS IN MAIN LOOP
C
135     IF(XNORMF-FNMIN) 800,136,136
136     IFIN=0
        IF(EPSILN-1.)137,138,137
137     EPSILN=1.
138     CONTINUE
```

```
C
C
C
      DO 139 I=1,N
      XKPL(I)=XK2(I)
      XK(I)=XKNEW(I)
139   CONTINUE
      FKLAST=XNORMF
      FKBF4=XNORMF
      PRINT 140,IPASS,(XK(I),I=1,N)
140   FORMAT(6H PASS=,I3,5H KXY= ,6(E12.5,1X)///)
      PRINT 114,EPSILN
      GO TO 100
800   CONTINUE
      CALL ACCEPT( XKNEW,IGOOD)
      IF(IGOOD)802,802,803
802   PRINT  904,((I,XKNEW(I)),I=1,N)
904   FORMAT(1H ,/,16H SOLUTION IS BAD    ,6(3H K(,I2,2H)=,E12.5,/))
      IBAD=1
      GO TO 811
803   PRINT  900,((I,XKNEW(I)),I=1,N)
900   FORMAT(1H ,/,17H SOLUTION IS GOOD   ,6(3H K(I1,2H)=,E12.5,/))
      GO TO 811
801   PRINT  902
902   FORMAT(11H 100 PASSES      )
811   CONTINUE
      INORM=INORM+1
C     CHECK DIFFERENT NORM COMPUATION
      IF(INORM-2) 830,830,812
812   CONTINUE
      RETURN
      END
      SUBROUTINE DECOMP(N,NDIM,A,IP)
      DIMENSION A(6,6),IP(6)
C
C     CACM ALGORITHM 423 USED WITH SOLVE
C
C     LINEAR EQUATION SOLVER USING LU DECOMPOSITION
C
      COMMON A12,A21,B1,Y1F,Y3F,ETA
      IP(N)=1
      DO 6 K=1,N
        IF(K-N) 55,5,55
55    CONTINUE
        KP1=K+1
        M=K
        DO 1 I=KP1,N
          IF(ABSF(A(I,K))-ABSF(A(M,K)))1,1,11
11        M=I
1       CONTINUE
        IP(K)=M
        IF(M-K) 20,21,20
20      IP(N)=-IP(N)
21      CONTINUE
        T=A(M,K)
        A(M,K)=A(K,K)
```

```
          A(K,K)=T
          IF(T)23,5,23
23        CONTINUE
          DO 2 I=KP1,N
2           A(I,K)=-A(I,K)/T
          DO 4 J=KP1,N
            T=A(M,J)
            A(M,J)=A(K,J)
            A(K,J)=T
            IF(T)33,4,33
33          CONTINUE
            DO 3 I=KP1,N
3             A(I,J)=A(I,J)+A(I,K)*T
4         CONTINUE
5         IF(A(K,K))6,66,6
66          IP(N)=0
6       CONTINUE
        RETURN
        END
        SUBROUTINE SOLVE(N,NDIM,A,B,IP)
C
C       LINEAR EQUATION SOLVER USING LU DECOMPOSITION
C
C       CACM ALGORITHM 423 USED WITH DECOMP
C
        DIMENSION A(6,6),B(6),IP(6)
        COMMON A12,A21,B1,Y1F,Y3F,ETA
        IF(N-1) 99,9,99
99      NM1=N-1
        DO 7 K=1,NM1
          KP1=K+1
          M=IP(K)
          T=B(M)
          B(M)=B(K)
          B(K)=T
          DO 7 I=KP1,N
7       B(I)=B(I)+A(I,K)*T
        DO 8 KB=1,NM1
          KM1=N-KB
          K=KM1+1
          B(K)=B(K)/A(K,K)
          T=-B(K)
          DO 8 I=1,KM1
8       B(I)=B(I)+A(I,K)*T
9       B(1)=B(1)/A(1,1)
        RETURN
        END
```

VITA

Mr. John Peter Schill was born on February 3, 1943 in Chicago, Illinois. He received his primary and secondary education in Chicago, graduating from Senn High School in June 1960.

While attending the University of Illinois, he earned Bachelor of Science degrees in Electrical Engineering and Psychology in 1965. He earned a Master of Science degree in Electrical Engineering in 1969 from the University of Illinois.

From September 1965 to June 1968, he was employed as a research and teaching assistant at the University of Illinois. In 1968, he was employed at the University of North Carolina as a research associate, and in 1969, he was employed at the University of California - San Diego, as a postgraduate research bioengineer, while working with the same patient monitoring research group.

In 1970 he started work for the Naval Electronics Laboratory Center. Although he has been occasionally involved with biomedical research projects there, he is presently engaged in telecommunications architecture and multiple processor design.